Regenerative Therapy 31 (2026) 101049

Contents lists available at ScienceDirect

Regenerative Therapy

journal homepage: www.elsevier.com/locate/reth

Hypoxia-preconditioned bone marrow mesenchymal stem cell-derived exosomes ameliorate knee osteoarthritis by promoting cartilage regeneration and alleviating pain in rats

Binbin Zhang, Chuan Lu, Bin Dou, Wenzuo Gu, Kewen Li *

Department of Orthopedics and Joint Surgery, Qinghai University Affiliated Hospital, Qinghai University, Xining, Qinghai, 810000, China

ARTICLE INFO

Keywords:
Osteoarthritis
BMSCs
Hypoxic
Exosomes
Cartilage

ABSTRACT

Objective: Knee osteoarthritis (KOA) is the most prevalent subtype of arthritis, characterized by progressive degeneration of articular cartilage. The present study aimed to investigate the reparative potential of exosomes derived from hypoxia-preconditioned bone marrow mesenchymal stem cells (Hypo-BMSCs-Exos) in treating cartilage damage associated with KOA.

Methods: An in vitro KOA chondrocyte model was established through induction with interleukin-1β (IL-1β). Subsequently, the modeled chondrocytes were co-cultured with Hypo-BMSCs-Exos. Flow cytometry, Western blotting, immunofluorescence staining, and senescence-associated β-galactosidase (SA-β-gal) staining were used to evaluate the effects of Hypo-BMSCs-Exos on chondrocyte proliferation, apoptosis, extracellular matrix (ECM) metabolic homeostasis, and cellular senescence. For in vivo assessment of Hypo-BMSCs-Exos efficacy, exosomes were administered to KOA model rats via intra-articular injection. Histological scoring, Micro-CT, pain behavioral assessments, and immunohistochemical analysis were then performed to determine the reparative effects of Hypo-BMSCs-Exos on cartilage damage.

Results: Hypo-BMSCs-Exos exerted superior effects in suppressing inflammatory responses, apoptosis, ECM degradation, and cellular senescence in rat chondrocytes. Specifically, treatment with Hypo-BMSCs-Exos upregulated the expression of ECM synthesis-related proteins (Collagen II, aggrecan) while downregulating the expression of ECM degradation-related proteins (ADAMTS-5, MMP-13), pro-inflammatory cytokines (iNOS, COX2), and key senescence-associated proteins (p53, p21, p16). Additionally, a reduction in the number of SA-β-gal-positive senescent chondrocytes was observed. In vivo experiments revealed that intra-articular injection of Hypo-BMSCs-Exos in KOA rats significantly improved the inflammatory microenvironment within the joint, promoted articular cartilage regeneration, and restored the structural integrity of subchondral bone. Furthermore, in vivo findings demonstrated that Hypo-BMSCs-Exos significantly regulated the expression of pain-related molecules and exerted a marked inhibitory effect on pain-related behaviors in KOA rats.

Conclusion: Hypo-BMSCs-Exos can effectively alleviate cartilage degeneration and pain in KOA, thus offering a novel and promising cell-free therapeutic strategy for the intervention of KOA.

1. Introduction

Knee osteoarthritis (KOA) is a degenerative joint disease characterized by cartilage degeneration, synovial inflammation, and osteophyte formation [1,2]. The global incidence of KOA has been rising annually. Statistics indicate that the number of KOA patients worldwide reached 374 million in 2021 [3]; additionally, the proportion of young individuals with early-onset osteoarthritis is also on the increase [4]. Currently, the primary goals of clinical treatment for KOA are to relieve symptoms and slow disease progression. Common treatment options include analgesia with nonsteroidal anti-inflammatory drugs (NSAIDs), intra-articular drug injection, and total joint replacement for end-stage disease [5–7]. However, long-term use of NSAIDs tends to cause gastrointestinal damage and elevate cardiovascular risks [8]. The

Peer review under responsibility of the Japanese Society for Regenerative Medicine.

* Corresponding author. Department of Orthopedics and Joint Surgery, Qinghai University Affiliated Hospital, Qinghai University, 29 Tongren Road, Xining, Qinghai, 810000, China.

E-mail address: qdfykwl@126.com (K. Li).

https://doi.org/10.1016/j.reth.2025.101049

Received 11 October 2025; Received in revised form 8 November 2025; Accepted 26 November 2025

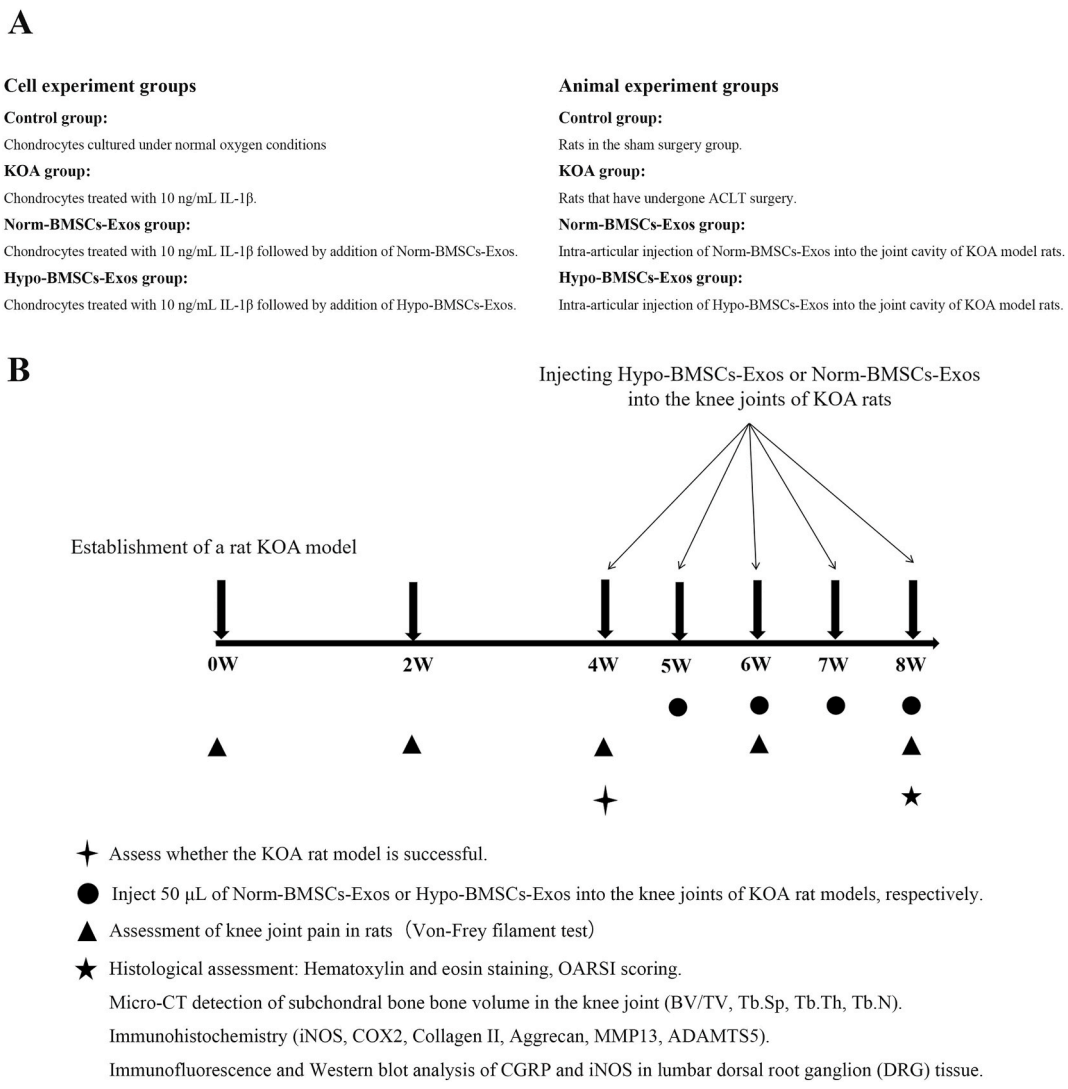

Fig. 1. Flow chart.
A: Grouping of animal experiments and cell experiments in this study. **B:** The schedule for injecting BMSCs-Exos into the joint cavity of KOA rats and different detection methods after injection.

efficacy of intra-articular hyaluronic acid injection varies among individuals: it only relieves knee pain in the short term and fails to reverse cartilage degeneration [9]. Although total joint replacement improves joint function, it is associated with extensive surgical trauma and high costs, making it unsuitable for young patients [10]. Therefore, exploring safe and effective new therapeutic strategies for KOA has become a research focus in the field of orthopedics.

Mesenchymal stem cells (MSCs) have shown considerable potential in tissue repair due to their multi-directional differentiation capacity and immunomodulatory properties [11,12]. However, in clinical research, issues such as immune rejection, tumor formation related to cell transplantation, and vascular embolism still limit the clinical application of MSCs. MSCs primarily participate in tissue repair by releasing bioactive substances through paracrine signaling [13]. Among these substances, exosomes can carry microRNAs (miRNAs), proteins, and lipids to mediate intercellular communication. Thus, they are regarded as the main effector molecules underlying the therapeutic effects of MSCs [14,15]. Researchers have found that injecting bone marrow mesenchymal stem cell-derived exosomes (BMSCs-Exos) into a rat KOA model can inhibit the expression of matrix metalloproteinases (MMPs) in chondrocytes and reduce the degradation of type II collagen and proteoglycans [16,17]. Meanwhile, BMSCs-Exos also suppress inflammatory damage and oxidative stress in chondrocytes [18]. These findings lay a foundation for the application of BMSCs-Exos as a "cell--free therapeutic strategy" for KOA.

Notably, BMSCs naturally reside in a hypoxic physiological microenvironment, whereas in vitro culture under normoxic conditions may diminish their biological activity. In recent years, studies have revealed that a hypoxic environment can enhance the proliferation ability and cytokine secretion efficiency of BMSCs by activating the HIF-1α signaling pathway [19]. On the other hand, the interior of knee joint cartilage is a physiologically hypoxic environment, with oxygen tension much lower than that in ambient air or arterial blood [20]. Therefore, it is reasonable to conclude that a hypoxic environment is more consistent with the physiological microenvironment of both BMSCs and chondrocytes. However, research on the relationship between hypoxia-preconditioned BMSC-derived exosomes (Hypo-BMSCs-Exos) and chondrocyte metabolism remains limited. It is currently unclear whether Hypo-BMSCs-Exos can achieve better therapeutic effects in KOA than BMSCs-Exos derived from normoxically cultured BMSCs (Norm-BMSCs-Exos).

Based on the aforementioned research status, we hypothesized that Hypo-BMSCs-Exos could more effectively alleviate cartilage degeneration in KOA. In this study, we first analyzed the activity and

differentiation ability of BMSCs cultured under normoxic and hypoxic conditions. Subsequently, we isolated and identified Norm-BMSCs-Exos and Hypo-BMSCs-Exos. Finally, we clarified the biological functions of Hypo-BMSCs-Exos in chondrocyte metabolic activities through relevant in vitro assays. We also established a rat KOA model to further explore the therapeutic effects of Hypo-BMSCs-Exos in improving knee cartilage defects, restoring joint function, and alleviating pain. This study may provide new insights and experimental basis for the treatment of KOA.

2. Materials and methods

2.1. Experimental animals

The overall study design and grouping are presented in Fig. 1. For this study, 12-week-old female Sprague-Dawley (SD) rats were purchased from Beijing SPF Biotechnology Co., Ltd. The rats were housed in a specific pathogen-free (SPF) facility, with free access to food and water provided throughout the study. Environmental conditions were maintained at the barrier-system level, with temperature ranging from 20 °C to 26 °C and relative humidity from 30 % to 70 %.

2.2. Culture and intervention of chondrocytes

Primary rat chondrocytes were purchased from iCell Bioscience Inc. (iCell, China). The chondrocytes were cultured in Dulbecco's Modified Eagle Medium (DMEM; BasalMedia, China) supplemented with 10 % fetal bovine serum (FBS; Vivacell, China) and 1 % penicillin-streptomycin solution (Biosharp, China). The culture incubator was maintained at 37 °C with 5 % CO_2. Chondrocytes were passaged when they reached 80 % confluence. To preserve the phenotype of primary chondrocytes, only passage 1 (P1) chondrocytes were used in this experiment. For the establishment of an in vitro KOA chondrocyte model, consistent with previous studies [21], chondrocytes were treated with 10 ng/mL interleukin-1β (IL-1β; MCE, USA)—a widely used method to simulate the in vitro inflammatory microenvironment of KOA.

2.3. Culture and identification of BMSCs

Rat bone marrow mesenchymal stem cells (BMSCs) were purchased from iCell Bioscience Inc. (iCell, China). BMSCs were cultured in DMEM (BasalMedia, China) supplemented with 10 % FBS (Vivacell, China) and 1 % penicillin-streptomycin solution (Biosharp, China), with incubation at 37 °C and 5 % CO_2. Flow cytometry was employed to identify BMSCs by detecting their surface-specific antigens, including CD29, CD34, CD45, and CD90 (all from BioLegend, USA).

2.4. Normoxic or hypoxic culture conditions for BMSCs

For well-grown third-passage (P3) BMSCs, the culture serum was replaced with 10 % exosome-free fetal bovine serum. As described in previous research [22], the hypoxic group was incubated in a tri-gas cell incubator (LTG-165T, Shanghai, China) for 24 h under conditions of 37 °C, 5 % CO_2, 1 % O_2, and 95 % saturated humidity. The normoxic group was cultured in a conventional incubator for 24 h, with the environment maintained at 37 °C, 5 % CO_2, 21 % O_2, and 95 % saturated humidity.

2.5. Directed differentiation of BMSCs

BMSCs from the normoxic and hypoxic groups were collected separately. The original culture medium was discarded, and osteogenic, chondrogenic, or adipogenic induction medium (all purchased from Procell, China) was added to induce differentiation. After induction, the cells were fixed with 4 % paraformaldehyde for 30 min, rinsed with phosphate-buffered saline (PBS), and then stained with Alizarin Red S (for osteogenic differentiation), Alcian Blue (for chondrogenic differentiation), or Oil Red O (for adipogenic differentiation) for 30 min. Images were captured under a light microscope.

2.6. Flow cytometric analysis of apoptosis

An Annexin V-APC/PI Double Staining Apoptosis Detection Kit (keyGEN, China) was used to detect apoptosis in BMSCs and chondrocytes. When cells in each group reached approximately 80 % confluence, they were stained using the Annexin V-APC/PI kit. The proportion of apoptotic cells was determined with a Beckman CytoFLEX flow cytometer (Beckman, USA).

2.7. Isolation of exosomes from BMSCs

Exosomes were isolated from BMSCs via differential centrifugation [23]. P3 BMSCs from the normoxic and hypoxic groups were collected separately. The cell culture supernatant was first centrifuged at 300×*g* for 10 min at 4 °C. The resulting supernatant was carefully aspirated and then centrifuged at 3000×*g* for 15 min at 4 °C to remove residual cell debris. The supernatant obtained from this step was transferred to a sterile centrifuge tube and further centrifuged at 10,000×*g* for 45 min at 4 °C to remove large vesicles. The supernatant was then filtered through a 0.45 μm membrane and ultracentrifuged at 100,000×*g* for 70 min at 4 °C using an ultracentrifuge rotor (CP100MX, Hitachi, Japan). The resulting pellet was resuspended in PBS, filtered through a 0.22 μm membrane, and subjected to ultracentrifugation again. The final pellet contained the target exosomes, which was resuspended in an appropriate volume of PBS and stored at −80 °C for subsequent experiments.

2.8. Identification of rat BMSC-derived exosomes

A 10 μL aliquot of exosome samples from either the normoxic or hypoxic group was dropped onto a copper grid and allowed to settle for 1 min. Excess liquid was blotted away with filter paper. A 10 μL aliquot of uranyl acetate (Zhongjing Keying Technology Co., Ltd, China) was then added to the copper grid and left to stand for 1 min. Excess liquid was blotted away again, and the grid was air-dried at room temperature for several minutes. The morphology of normoxic BMSC-derived exosomes (Norm-BMSCs-Exos) and hypoxic BMSC-derived exosomes (Hypo-BMSCs-Exos) was observed with a transmission electron microscope (Hitachi, Japan). Nanoparticle tracking analysis (NTA; Particle Metrix, Germany) was used to determine and analyze the diameter of the exosomes. To detect exosome markers, 50 μL of exosome suspension was incubated with primary antibodies against CD9 (Bio-techne, USA), CD63 (Abcam, UK), and CD81 (BioLegend, USA) for 30 min at 4 °C in the dark. After washing, the suspension was incubated with a pre-adsorbed secondary antibody (Abcam, UK) for 30 min at 4 °C in the dark, and flow cytometric analysis was then performed.

2.9. BCA assay for exosome protein concentration

The protein concentration of the exosomes was measured using a BCA Protein Assay Kit (Beyotime, China). Standard protein samples were prepared in accordance with the kit instructions. A 20 μL aliquot of the diluted exosome sample was added to the BCA working solution and mixed thoroughly. After incubation at 37 °C for 30 min, the absorbance was measured at 562 nm with a microplate reader. The protein concentration of the samples was calculated using the standard curve.

2.10. Tracking of rat BMSC-derived exosomes

PKH26 dye (Umibio, China) was prepared following the kit instructions, with the mixture composed of 1 μL PKH26 dye and 9 μL Diluent C. The PKH26 solution was added to either Norm-BMSCs-Exos or Hypo-BMSCs-Exos, mixed thoroughly, and incubated for 10 min at room

temperature in the dark. Excess fluorescent dye was removed via ultracentrifugation at 100,000×*g* for 1 h at 4 °C, and the labeled exosomes were then washed three times with PBS. After resuspension in PBS, PKH26-labeled Norm-BMSCs-Exos or Hypo-BMSCs-Exos (red fluorescence) were co-cultured with KOA chondrocytes for 24 h or 48 h, respectively. The culture plate was removed, and the supernatant was aspirated. The cells were washed twice with PBS, fixed with 4 % paraformaldehyde at room temperature for 30 min, and then washed three times with PBS. Cell nuclei were stained with DAPI (blue fluorescence) for 10 min, and images were captured with a fluorescence microscope (Olympus, Japan).

2.11. CCK-8 assay for chondrocyte proliferation

Chondrocytes were seeded into a 96-well plate and treated with 10 ng/mL interleukin-1β (IL-1β) for 24 h. Subsequently, 50 μg of either Norm-BMSCs-Exos or Hypo-BMSCs-Exos was added to each well, and the cells were cultured in an incubator maintained at 37 °C with 5 % CO_2. A 110 μL aliquot of CCK-8 working solution (Biosharp, China) was added to each well, and the plate was then incubated for 2 h. After 24 h and 48 h of culture, the absorbance at 450 nm was measured with a microplate reader to evaluate chondrocyte proliferation.

2.12. Western blotting analysis

For chondrocytes in different treatment groups, total proteins were extracted using pre-cooled RIPA lysis buffer (NCM Biotech, China) supplemented with a protease/phosphatase inhibitor cocktail (also from NCM Biotech, China). The protein concentration was determined using the BCA assay described above. Protein samples were separated by sodium dodecyl sulfate-polyacrylamide gel electrophoresis (SDS-PAGE; Biosharp, China) and then transferred to a 0.22 μm polyvinylidene difluoride (PVDF) membrane (Sigma-Aldrich, Germany) at a constant current of 300 mA. The membrane was blocked with 5 % non-fat milk for 1 h at room temperature. Primary antibodies against inducible nitric oxide synthase (iNOS; Affinity, USA; 1:2000), cyclooxygenase-2 (COX2; Huabio, China; 1:2000), type II collagen (Collagen II; Affinity, USA; 1:2000), aggrecan (Abclonal, USA; 1:1000), a disintegrin and metalloproteinase with thrombospondin motifs 5 (ADAMTS-5; Affinity, USA; 1:2000), matrix metalloproteinase 13 (MMP-13; Proteintech, USA; 1:1000), p16 (Abclonal, USA; 1:1000), p21 (Proteintech, USA; 1:2000), and p53 (Immunoway, USA; 1:2000) were incubated with the membrane overnight at 4 °C. After removing the primary antibody on ice, the membrane was washed three times with Tris-buffered saline containing Tween 20 (TBST) and then incubated with a horseradish peroxidase (HRP)-conjugated secondary antibody (Abclonal, USA) for 1 h at room temperature. Protein bands were visualized using an enhanced chemiluminescence (ECL) reagent (Biosharp, China) and imaged. β-actin served as the internal reference. The relative protein expression levels were quantified using ImageJ software (National Institutes of Health, USA).

2.13. Immunofluorescence staining

Chondrocytes in different treatment groups were fixed with 4 % paraformaldehyde for 15 min at room temperature. Permeabilization buffer was added to cover the cells and incubated for 10 min at room temperature. The cells were then washed three times with PBS, with each wash lasting 5 min. After blocking with bovine serum albumin (BSA) for 20 min at room temperature and subsequent washing with PBS, the cells were incubated overnight at 4 °C with primary antibodies against iNOS (Servicebio, China), COX2 (Servicebio, China), Collagen II (Bisso, China), aggrecan (Bisso, China), ADAMTS-5 (Bisso, China), MMP-13 (Affinity, USA), p16 (Abcam, USA), p21 (Affinity, USA), and p53 (Proteintech, USA). The following day, the cells were incubated with the corresponding fluorescent secondary antibodies for 1.5 h at 37 °C. Cell nuclei were stained with 4′,6-diamidino-2-phenylindole (DAPI; Servicebio, China) for 3 min at room temperature. The samples were observed and imaged with a fluorescence microscope (Olympus, Japan), and the fluorescence intensity was quantified using ImageJ software.

2.14. Senescence-associated β-galactosidase (SA-β-gal) staining

Senescence-associated β-galactosidase (SA-β-gal) staining was performed using a β-Galactosidase Staining Kit (Solarbio, China). For chondrocytes in different treatment groups, the supernatant in each well was aspirated, and the cells were washed three times with PBS. A 1 mL aliquot of β-galactosidase fixation solution was added, and the cells were fixed for 15 min at room temperature. After removing the fixation solution, the cells were washed twice with PBS, with each wash lasting 3 min. A 1 mL aliquot of staining working solution (prepared as follows: 10 μL β-galactosidase staining solution A, 10 μL β-galactosidase staining solution B, 930 μL β-galactosidase staining solution C, and 50 μL X-Gal solution) was added to each well. The cells were then incubated overnight at 37 °C. The cells were observed and imaged under a light microscope.

2.15. Intracellular reactive oxygen species (ROS) measurement

The culture medium in each well was aspirated, and the cells were gently washed twice with PBS pre-warmed to 37 °C. A total of 1 mL of serum-free medium containing the DCFH-DA probe (Beyotime, China) was added to each well, and the cells were incubated for 30 min at 37 °C in the dark. After incubation, the probe-containing medium was discarded, and the cells were washed twice with PBS to completely remove any free, uninternalized probe. Subsequently, 0.5 mL of trypsin was added to each well, and the cells were incubated at 37 °C for 2–3 min. When cell shrinkage and increased intercellular spacing were observed under a microscope, 1 mL of complete culture medium was added to terminate digestion. The cells were gently pipetted to form a single-cell suspension, which was then transferred to a 1.5 mL light-protected centrifuge tube. The suspension was centrifuged at 1000 rpm for 5 min, the supernatant was discarded, and the cell pellet was resuspended in PBS. This centrifugation and resuspension step was repeated once. Finally, the cells were resuspended in PBS, passed through a 300-mesh cell strainer, and transferred to a flow cytometry-compatible, light-protected tube. The ROS levels in different groups were measured with a flow cytometer.

2.16. Establishment of rat KOA model and intra-articular injection of exosomes

A rat KOA model was established using the methods described in previous studies [24–26]. Rats were anesthetized by intraperitoneal injection of 3 % sodium pentobarbital at a dose of 3 mL/kg body weight and then fixed in a supine position. Sham operation group (Control group): After shaving the hair on both hind limbs, the knee joint capsule was opened through a medial parapatellar approach, with the anterior cruciate ligament (ACL) left intact (i.e., not transected). KOA model group: After opening the knee joint capsule, the ACL was transected and the medial meniscus was excised. The muscles and skin were closed layer by layer. The affected hind limb was not immobilized, and the rats were housed in individual cages with free movement. For 3 days after surgery, each rat was intramuscularly injected with 0.1 mL of penicillin sodium injection (800,000 units/mL) once daily. To validate the effectiveness of the KOA model, three rats were randomly selected from the KOA model group for evaluation four weeks post-surgery. After successful model establishment, rats in the KOA group were randomly allocated into different treatment groups. The control and KOA groups received injections of normal saline, whereas the Norm-BMSCs-Exos and Hypo-BMSCs-Exos groups were administered 50 μg of

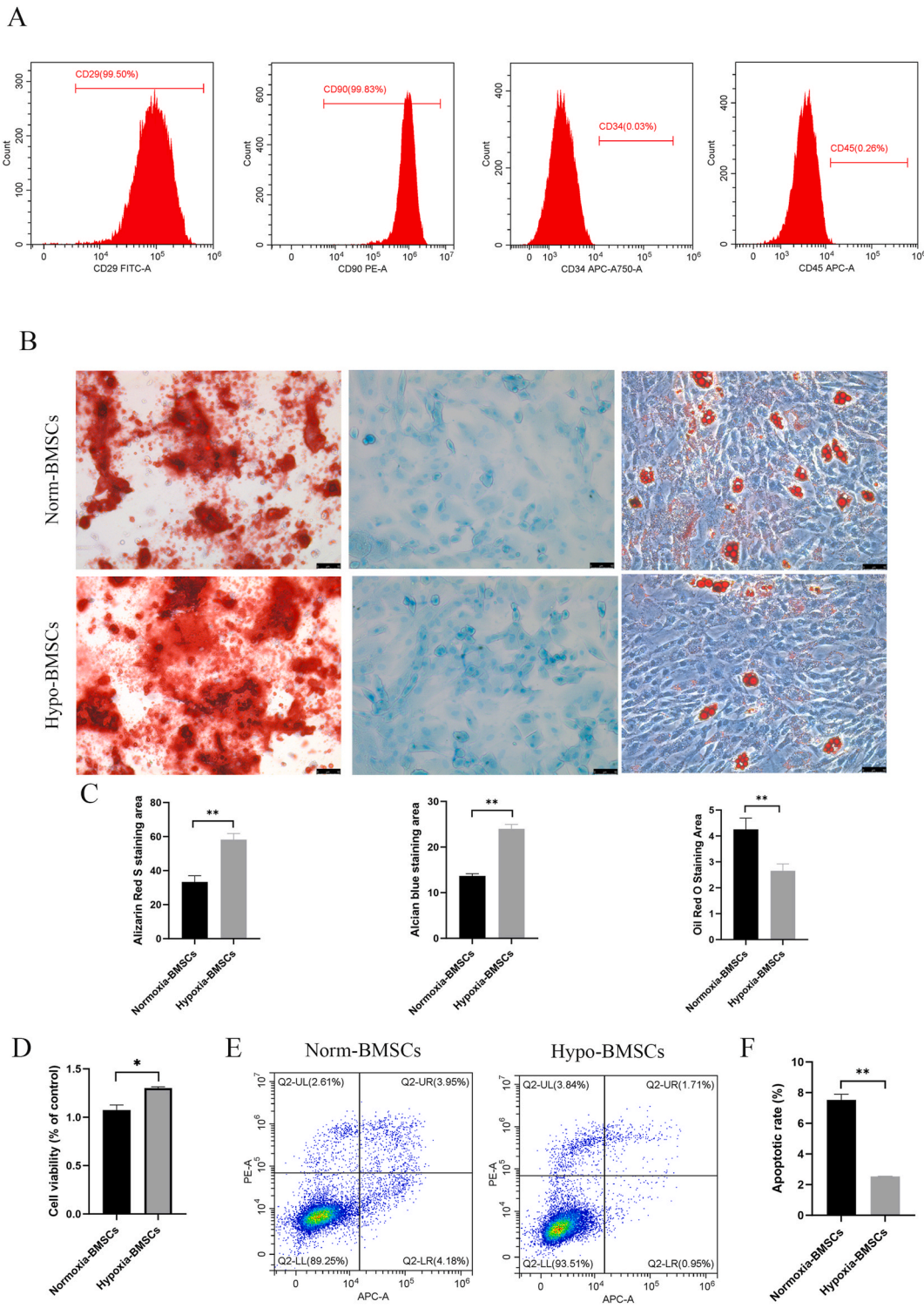

Fig. 2. Identification of BMSCs and biological changes in hypoxic conditions.
A: Expression of surface markers (CD90, CD29, CD34, CD45) on rat BMSCs analyzed by flow cytometry. **B:** Osteogenic, adipogenic, and chondrogenic differentiation of Norm-BMSCs and Hypo-BMSCs. Scale = 50 μm. **C:** Quantitative analysis of BMSC differentiation potential. Hypo-BMSCs exhibit enhanced osteogenic and chondrogenic differentiation capacity but reduced adipogenic differentiation. **D:** Proliferation assessment of Norm-BMSCs and Hypo-BMSCs via CCK-8 assay. **E:** Flow cytometry analysis of apoptosis in Norm-BMSCs and Hypo-BMSCs. F: Quantitative analysis of apoptosis in Norm-BMSCs and Hypo-BMSCs. Data are presented as Mean ± SD. Intergroup differences with statistical significance: *P < 0.05, **P < 0.01, n = 3 per group.

Norm-BMSCs-Exos or Hypo-BMSCs-Exos, respectively. Injections were performed twice weekly for a total duration of five weeks. This dosing regimen for Norm-BMSCs-Exos and Hypo-BMSCs-Exos has previously been demonstrated to be effective in animal models of osteoarthritis [27]. At the eighth week, all rats were euthanized via anesthetic overdose, and knee joint samples were collected for subsequent assessment of disease progression.

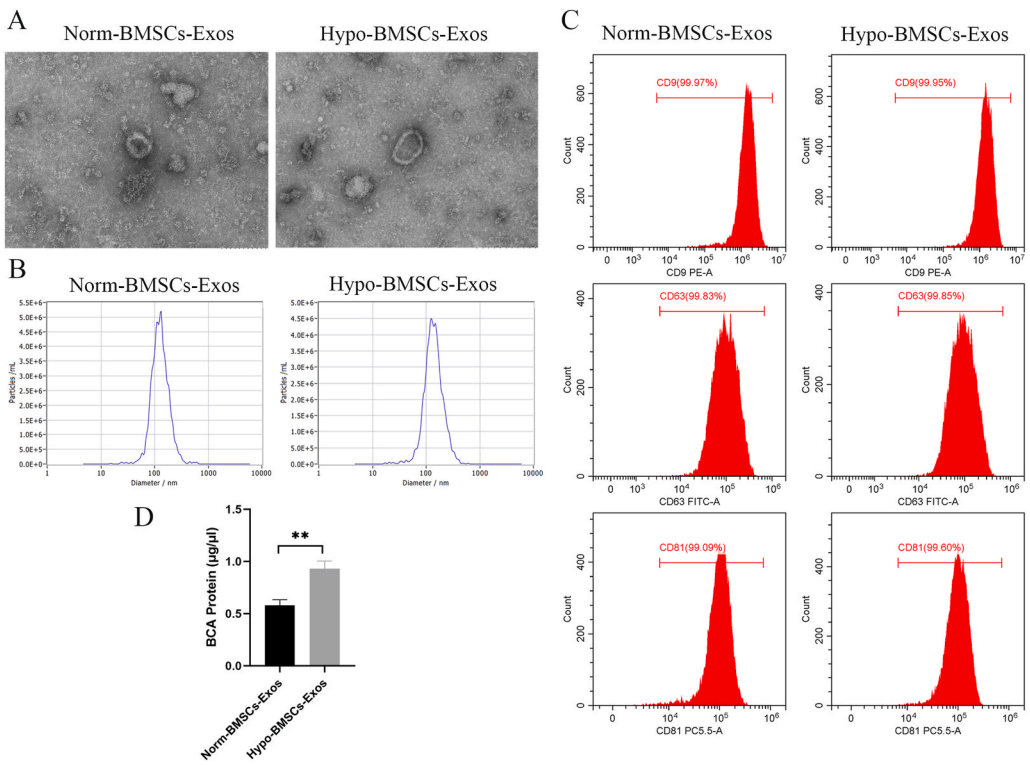

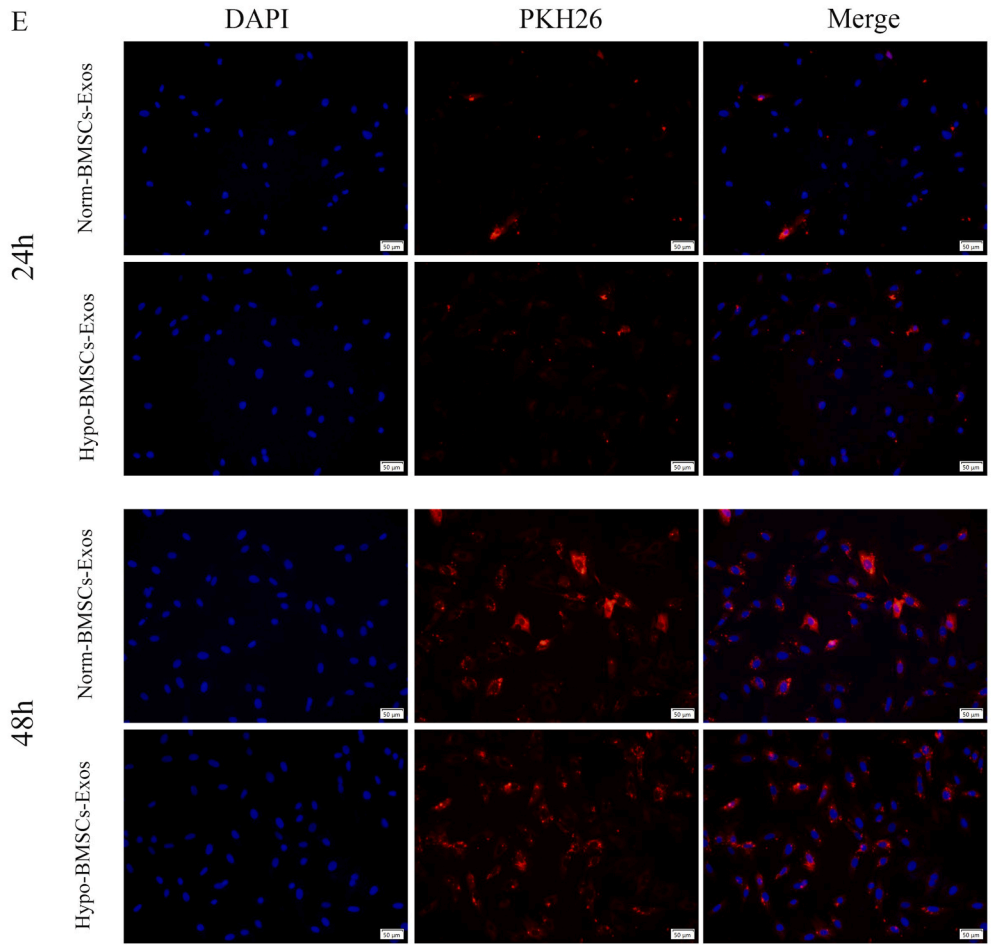

(caption on next page)

Fig. 3. Characterization of hypoxic and normoxic pretreated BMSCs-Exos.
A: Morphology of Norm-BMSCs-Exos and Hypo-BMSCs-Exos under transmission electron microscopy. **B:** Nanoparticle tracking analysis (NTA) of Norm-BMSCs-Exos and Hypo-BMSCs-Exos reveals similar size distributions (40–160 nm). **C:** Flow cytometry analysis of surface marker expression (CD9, CD63, CD81) in Norm-BMSCs-Exos and Hypo-BMSCs-Exos. **D:** BCA assay was used to measure exosome protein concentration in Norm-BMSCs-Exos and Hypo-BMSCs-Exos. **E:** PKH26-labeled Norm-BMSCs-Exos and Hypo-BMSCs-Exos were internalized by chondrocytes. Data are presented as Mean ± SD. Intergroup differences were statistically significant at: *P < 0.05, n = 3 per group.

2.17. Histological evaluation

At week 8, joint tissues from rats in different groups were fixed in 10 % formaldehyde for 24 h, followed by decalcification in 10 % ethylenediaminetetraacetic acid (EDTA) solution at 37 °C for 7 days. The tissues were then dehydrated, embedded in paraffin, and sectioned into 5 μm-thick slices. The sections were stained with Safranin O-Fast Green. Two examiners independently graded the severity of cartilage damage on the medial tibial plateau of each specimen using the Osteoarthritis Research Society International (OARSI) histopathological scoring system [28]. Both examiners were blinded to the group assignments to avoid bias. A high-resolution microcomputed tomography (micro-CT) scanner (VivaCT 40; Scanco Medical AG, Switzerland) was used for imaging. Micro-CT images of the femoral and tibial articular surfaces (at a depth of approximately 1.5 mm) were imported into Image-Pro Plus software (Version 6.0.0; Media Cybernetics Inc., USA) to generate three-dimensional reconstructed images. Bone volume/total volume (BV/TV), trabecular pattern factor (Tb. Pf), trabecular separation (Tb. Sp), and trabecular number (Tb. N) were measured for comparative analysis.

2.18. Immunohistochemistry

Paraffin sections were deparaffinized to water and then subjected to antigen retrieval using a citrate buffer (pH 6.0). The sections were blocked with 10 % fetal bovine serum (FBS) for 1 h at room temperature, then incubated overnight at 4 °C with primary antibodies against iNOS (Servicebio, China), COX2 (ProteinTech Group, China), Collagen II (Bioss, China), aggrecan (Bioss, China), MMP-13 (ProteinTech Group, China), and ADAMTS-5 (Zenbio, China). The following day, the sections were incubated with the corresponding secondary antibodies for 1 h at 37 °C. After gentle washing with PBS and air-drying, fresh 3,3′-diaminobenzidine (DAB) chromogen solution was added to the sections for color development at room temperature (positive signals appeared brown). Cell nuclei were counterstained with hematoxylin for 5 min. The sections were sequentially immersed in 75 %, 85 %, 95 %, and absolute ethanol, each for 10 min, followed by immersion in xylene for 10 min. They were then mounted with neutral balsam. The percentage of the positive staining area was quantified using the Halo image analysis system (Indica Labs, USA).

2.19. Pain assessment

Previous studies have demonstrated that the Von Frey filament test can detect mechanical hyperalgesia in rats [29,30]. The 'up-down method' was used to test Von Frey filaments of different weights, and the hind paw withdrawal frequency in response to mechanical stimulation was recorded. This method assesses secondary mechanical hyperalgesia, a behavioral indicator of central and peripheral sensitization in KOA, where pain sensitivity is increased beyond the directly affected joint. To evaluate whether Hypo-BMSCs-Exos alleviate knee pain in rats, pain-related behaviors of KOA rats were assessed at weeks 2, 4, 6, and 8. Each rat was placed on a metal mesh grid, and Von Frey filaments were applied to the plantar surface of the hind paw. Paw withdrawal responses were recorded. Calcitonin gene-related peptide (CGRP) is a neuropeptide released by sensory neurons. In KOA, elevated CGRP levels are closely associated with pain sensitization and disease progression. In this study, Western blotting and immunofluorescence staining were used to detect the expression levels of CGRP and iNOS in the lumbar dorsal root ganglia (DRG).

2.20. Statistical analysis

All data in this study were analyzed using SPSS 25.0 statistical software, and statistical graphs were generated with GraphPad Prism 6.0 software. Quantitative data were expressed as mean ± standard deviation (mean ± SD). Two-group comparisons: If the data conformed to a normal distribution and exhibited homogeneous variance, an independent samples *t*-test was used; if the data were skewed (did not follow a normal distribution), non-parametric tests were employed. Multi-group comparisons: If the data conformed to a normal distribution and exhibited homogeneous variance, one-way analysis of variance (ANOVA) was used, followed by Tukey's post-hoc test for multiple comparisons; otherwise, the Kruskal-Wallis test was used, with the Bonferroni method for post-hoc analysis.

3. Results

3.1. Identification of rat BMSCs and biological changes of rat BMSCs under hypoxic conditions

First, rat bone marrow mesenchymal stem cells (BMSCs) were identified. Flow cytometric analysis showed that BMSCs highly expressed the surface markers CD29 (99.50 %) and CD90 (99.83), while the expression levels of CD34 (0.03 %) and CD45 (0.26 %) were low. This indicated that highly purified BMSCs were obtained in vitro (Fig. 2A). To assess whether a hypoxic environment affects the biological behavior of BMSCs, Alizarin Red S, Oil Red O, and Alcian Blue staining were used to compare the differentiation capacity of BMSCs cultured under normoxic conditions (Norm-BMSCs) and hypoxic conditions (Hypo-BMSCs) (Fig. 2B and C). Under appropriate induction conditions, Hypo-BMSCs exhibited a stronger ability to differentiate into osteoblasts and chondrocytes than Norm-BMSCs, but a weaker ability to differentiate into adipocytes. Results from the CCK-8 assay showed that Hypo-BMSCs had a more significant proliferation rate (Fig. 2D). Further detection via flow cytometry revealed that Hypo-BMSCs had a lower apoptosis rate (Fig. 2E and F). These findings suggest that a hypoxic environment may alter the biological activity of BMSCs, giving them a greater advantage in differentiating into chondrocytes and osteoblasts.

3.2. Identification and characterization of Norm-BMSCs-Exos and Hypo-BMSCs-Exos

In this study, normoxic BMSC-derived exosomes (Norm-BMSCs-Exos) and hypoxic BMSC-derived exosomes (Hypo-BMSCs-Exos) were first identified. Via transmission electron microscopy, both types of exosomes were observed to present as round or oval vesicles with a distinct phospholipid bilayer membrane structure (Fig. 3A). Nanoparticle tracking analysis (NTA) results showed that Norm-BMSCs-Exos and Hypo-BMSCs-Exos had similar size distributions, with diameters ranging from 40 to 160 nm (Fig. 3B), indicating no significant difference in the morphology of exosomes between the two groups. Flow cytometry was used to detect three extracellular surface molecular markers of exosomes, and the results showed high expression of CD9, CD63, and CD81 in both exosome groups (Fig. 3C). The BCA protein assay revealed that the total protein concentration of Hypo-BMSCs-Exos was

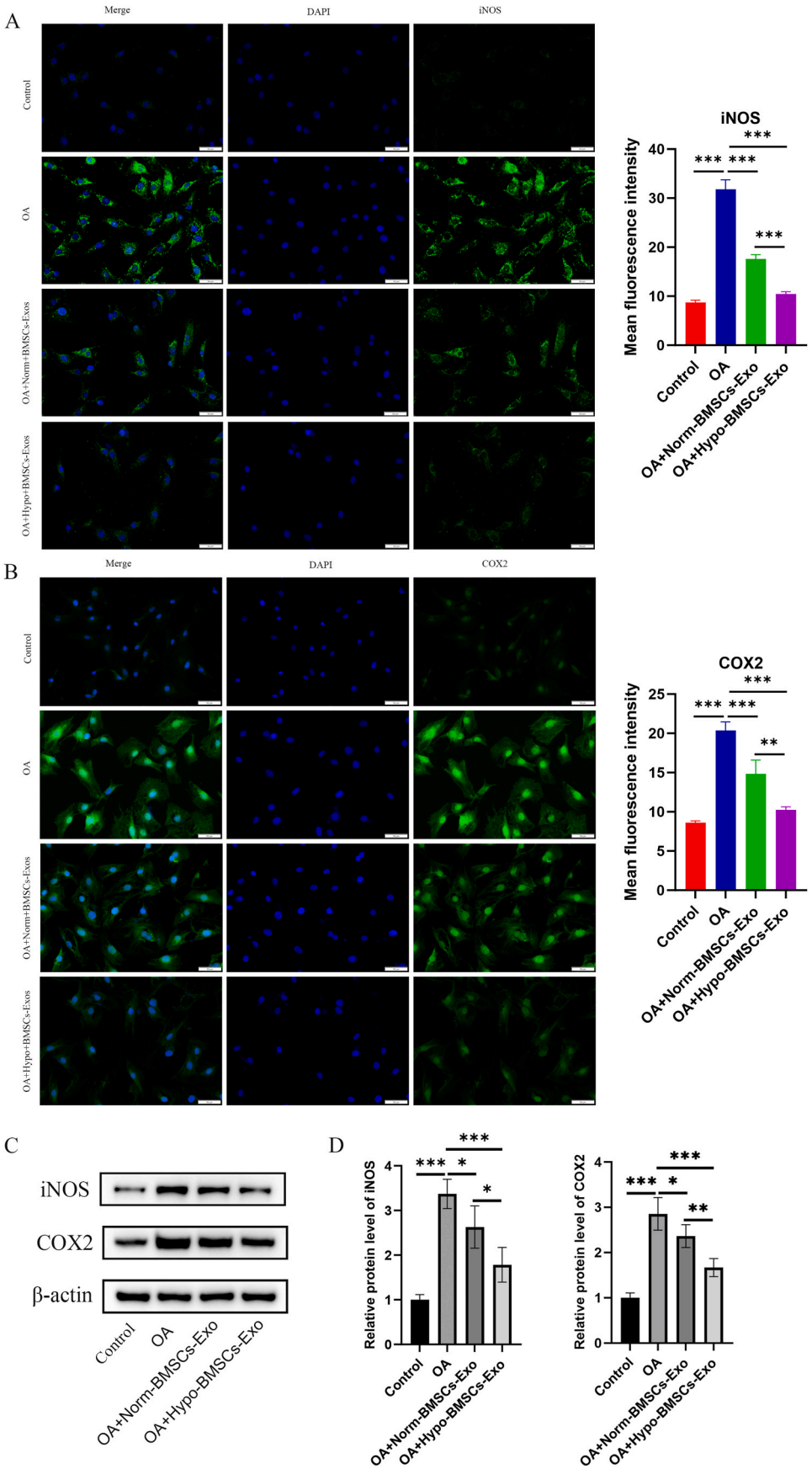

(caption on next page)

Fig. 4. Hypo-BMSCs-Exos attenuate IL-1β-Induced Chondrocyte Inflammation.
A: Immunofluorescence staining reveals changes in iNOS, and COX2 in IL-1β-induced chondrocytes following intervention with Norm-BMSCs-Exos and Hypo-BMSCs-Exos. **B:** Quantitative analysis of immunofluorescence staining. **C:** Western blot detection of protein expression levels of iNOS, and COX2 in IL-1β-induced chondrocytes treated with Norm-BMSCs-Exos and Hypo-BMSCs-Exos. **D:** Statistical analysis of relative protein band intensity values. Data are presented as Mean ± SD. Intergroup differences with statistical significance: *P < 0.05, **P < 0.01, ***P < 0.001, n = 3 per group.

significantly higher than that of Norm-BMSCs-Exos (Fig. 3D). Since the phagocytosis of exosomal informational substances by chondrocytes is critical for therapeutic efficacy, exosomes were stained with PKH26 dye and co-cultured with chondrocytes to verify whether Hypo-BMSCs-Exos can enter chondrocytes. Norm-BMSCs-Exos and Hypo-BMSCs-Exos labeled with the red fluorescent dye PKH26 were added to chondrocytes, and the results showed that both types of exosomes could be internalized by chondrocytes and localized in the cytoplasm surrounding the cell nucleus (Fig. 3E). In addition, changes in exosome uptake by chondrocytes at different time points (24 h and 48 h) were measured, and a significant increase in intracellular exosome uptake was observed at 48 h (Fig. 3E).

3.3. Hypo-BMSCs-Exos inhibit IL-1β-induced inflammation in chondrocytes

An in vitro KOA chondrocyte model was established using interleukin-1β (IL-1β) stimulation, consistent with previous studies. After IL-1β intervention, the proliferation of chondrocytes was decreased (Fig. S1A), whereas their apoptosis was increased (Fig. S1B). Norm-BMSCs-Exos or Hypo-BMSCs-Exos were co-cultured with IL-1β-stimulated chondrocytes for 24 h and 48 h, respectively. The results showed that Hypo-BMSCs-Exos had a more potent promotional effect on the proliferation of KOA chondrocytes than Norm-BMSCs-Exos. This proliferative effect became more pronounced as the treatment duration was prolonged, showing a time-dependent pattern. Therefore, a 48 h co-culture duration was used in subsequent experiments. Hypo-BMSCs-Exos effectively inhibited IL-1β-induced apoptosis in KOA chondrocytes, and this anti-apoptotic effect was stronger than that of Norm-BMSCs-Exos. These results suggest that hypoxic preconditioning may enhance the ability of BMSCs-Exos to inhibit KOA chondrocyte apoptosis by regulating their cargo content.

Excessive activation of inflammatory responses is a key pathological feature of chondrocyte damage. Inducible nitric oxide synthase (iNOS) and cyclooxygenase-2 (COX2) are critical effector molecules in inflammatory signaling pathways, and their expression levels directly reflect the inflammatory status of cells. Immunofluorescence results showed that the fluorescence intensities of iNOS and COX2 were increased in chondrocytes of the KOA model group, while they were decreased in both the Norm-BMSCs-Exos and Hypo-BMSCs-Exos groups—with a more significant reduction in the Hypo-BMSCs-Exos group (Fig. 4A and B). Western blot analysis revealed that compared with the control group, the protein expression levels of iNOS and COX2 in chondrocytes were significantly elevated in the KOA model group. After treatment with Norm-BMSCs-Exos, the protein expression levels of iNOS and COX2 were lower than those in the KOA model group. Moreover, the Hypo-BMSCs-Exos group showed a further downregulation of iNOS and COX2 protein expression, which was significantly lower than that in the Norm-BMSCs-Exos group. These results indicate that Hypo-BMSCs-Exos can more effectively suppress IL-1β-induced inflammatory responses in chondrocytes (Fig. 4C and D).

3.4. Effects of Hypo-BMSCs-Exos on the expression of cartilage matrix-related proteins in IL-1β-induced KOA chondrocytes

The core pathological feature of KOA is the imbalance between the degradation and anabolism of articular cartilage. Collagen II and aggrecan are core components of the cartilage matrix, and their degradation and loss are key pathological changes in cartilage damage. Matrix metalloproteinase 13 (MMP-13) and a disintegrin and metalloproteinase with thrombospondin motifs 5 (ADAMTS-5) are critical enzymes mediating cartilage matrix degradation; their overexpression is a major driver of progressive cartilage damage. Immunofluorescence results (Fig. 5A and B) showed that after 24 h of IL-1β-induced damage, the fluorescence intensities of ADAMTS-5 and MMP-13 in chondrocytes were increased, while those of Collagen II and aggrecan were decreased. After the addition of Norm-BMSCs-Exos or Hypo-BMSCs-Exos, the fluorescence intensities of ADAMTS-5 and MMP-13 were reduced, and those of Collagen II and aggrecan were elevated. Notably, Hypo-BMSCs-Exos induced a more significant decrease in the fluorescence intensities of ADAMTS-5 and MMP-13, as well as a more prominent increase in the fluorescence intensities of Collagen II and aggrecan. Western blot analysis (Fig. 5C and D) showed that compared with normal chondrocytes, the protein expression levels of ADAMTS-5 and MMP-13 were increased, while those of Collagen II and aggrecan were decreased in the IL-1β-induced KOA chondrocyte model. In contrast to the KOA model group, chondrocytes treated with Norm-BMSCs-Exos or Hypo-BMSCs-Exos exhibited increased protein expression of Collagen II and aggrecan, along with decreased protein expression of ADAMTS-5 and MMP-13. Specifically, the expression levels of MMP-13 and ADAMTS-5 in the Hypo-BMSCs-Exos group were significantly lower than those in the Norm-BMSCs-Exos group, while the expression levels of Collagen II and aggrecan were significantly higher. These results suggest that Hypo-BMSCs-Exos more effectively promote the recovery of matrix synthesis function in damaged chondrocytes and alleviate IL-1β-induced cartilage matrix destruction by inhibiting the expression of matrix-degrading enzymes.

3.5. Hypo-BMSCs-Exos delay IL-1β-induced senescence of chondrocytes

To further explore the effect of Hypo-BMSCs-Exos on the senescence of KOA chondrocytes, the senescence status of chondrocytes in different treatment groups was evaluated via senescence-associated β-galactosidase (SA-β-gal) staining and flow cytometry analysis. Immunofluorescence results showed that after IL-1β treatment, the fluorescence intensities of the senescence-related proteins p16, p21, and p53 in chondrocytes were significantly increased (Fig. 6A and B), indicating that IL-1β induced chondrocyte senescence. When Norm-BMSCs-Exos or Hypo-BMSCs-Exos were co-cultured with IL-1β-treated chondrocytes, the fluorescence intensities of p16, p21, and p53 showed a decreasing trend—with a more pronounced reduction in the Hypo-BMSCs-Exos co-culture group. Western blot analysis confirmed this observation: the protein expression levels of p16, p21, and p53 were increased in IL-1β-treated chondrocytes, and this trend was reversed by the addition of Norm-BMSCs-Exos or Hypo-BMSCs-Exos. Hypo-BMSCs-Exos exerted a more significant inhibitory effect on the expression of these senescence-related proteins (Fig. 6C and D). To visually observe the effect of Hypo-BMSCs-Exos on chondrocyte senescence, an SA-β-gal staining kit was used to detect SA-β-gal activity in chondrocytes (Fig. 6E and F). The results showed that IL-1β significantly increased the number of SA-β-gal-positive cells, while Hypo-BMSCs-Exos effectively inhibited SA-β-gal activity in chondrocytes. At the morphological level, this confirmed that Hypo-BMSCs-Exos can significantly suppress IL-1β-induced chondrocyte senescence. Cellular senescence is often accompanied by high levels of oxidative stress. Flow cytometry results showed that IL-1β increased the intracellular reactive oxygen species (ROS) levels in chondrocytes, whereas the addition of Hypo-BMSCs-Exos led to a more substantial reduction in ROS expression (Fig. 6G and H). In conclusion, Hypo-

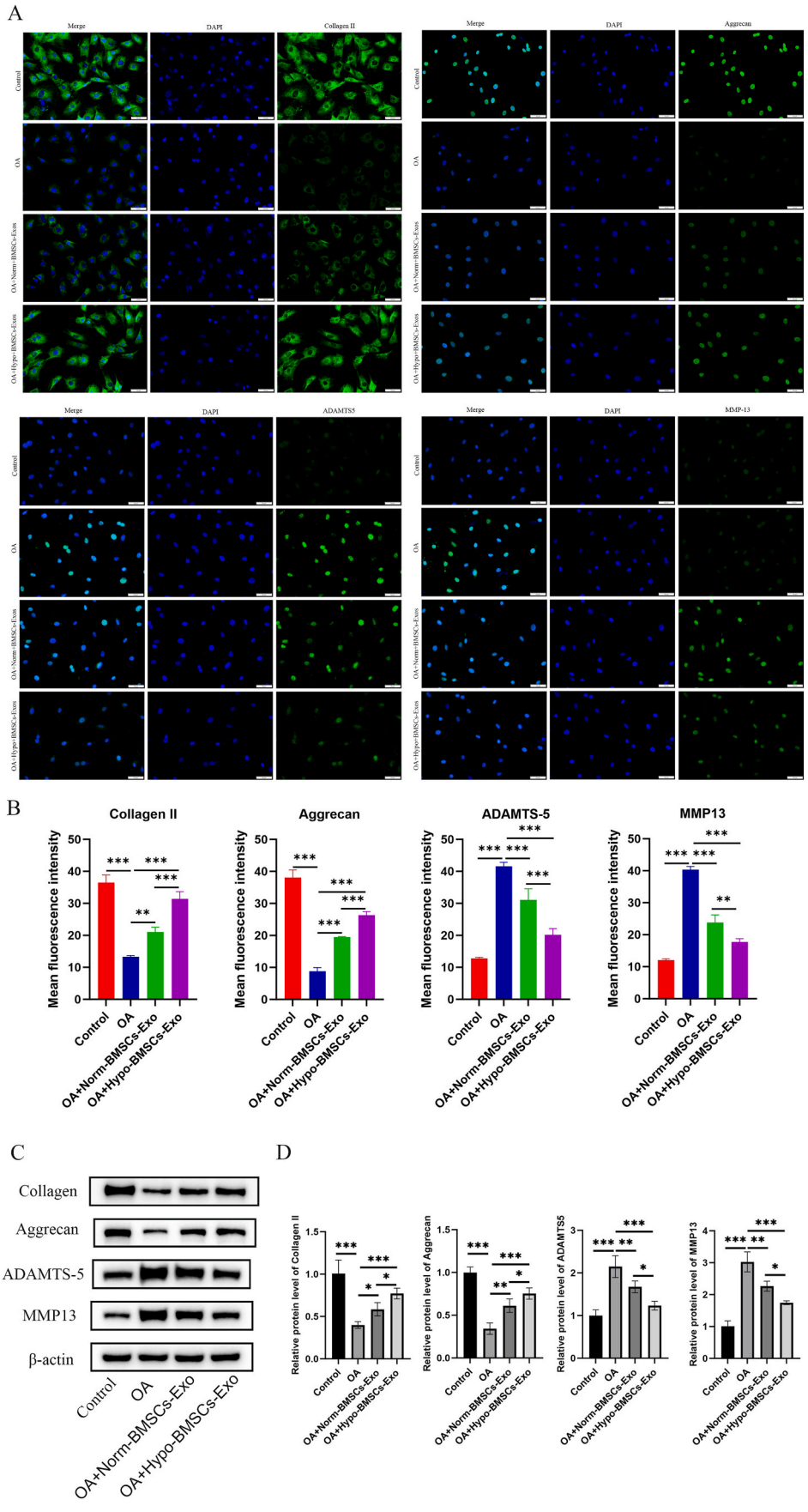

(caption on next page)

Fig. 5. Hypo-BMSCs-Exos attenuate IL-1β-induced chondrocyte injury.
A: Immunofluorescence staining reveals changes in Collagen II, Aggrecan, ADAMTS-5, and MMP-13 in IL-1β-induced chondrocytes following intervention with Norm-BMSCs-Exos and Hypo-BMSCs-Exos. **B:** Quantitative analysis of immunofluorescence staining. **C:** Western blot detection of protein expression levels of Collagen II, Aggrecan, ADAMTS-5, and MMP-13 in IL-1β-induced chondrocytes treated with Norm-BMSCs-Exos and Hypo-BMSCs-Exos. **D:** Statistical analysis of relative protein band intensity values. Data are presented as Mean ± SD. Intergroup differences with statistical significance: *P < 0.05, **P < 0.01, ***P < 0.001, n = 3 per group.

BMSCs-Exos can delay IL-1β-induced senescence of chondrocytes.

3.6. Intra-articular injection of Hypo-BMSCs-Exos delays articular cartilage degeneration in KOA rats

To investigate the effect of Hypo-BMSCs-Exos on articular cartilage degeneration in KOA rats, a rat KOA model was established by transecting the anterior cruciate ligament (ACL) and excising the medial meniscus. Norm-BMSCs-Exos and Hypo-BMSCs-Exos were then injected into the knee joint cavity of the model rats, respectively. The results showed that the cartilage surface in the KOA model group exhibited erosion and fissures, with a reduction in the number of chondrocytes in the damaged area and weakened matrix staining. In contrast, compared with the KOA model group, the degree of cartilage tissue damage was significantly alleviated in the Norm-BMSCs-Exos and Hypo-BMSCs-Exos injection groups—with Hypo-BMSCs-Exos promoting better recovery of cartilage tissue damage (Fig. 7A). The Osteoarthritis Research Society International (OARSI) histopathological scoring system was used for quantitative evaluation of cartilage degeneration. The results showed that the OARSI scores of the Norm-BMSCs-Exos and Hypo-BMSCs-Exos groups were lower than that of the KOA model group, and the OARSI score of the Hypo-BMSCs-Exos group was significantly lower than that of the Norm-BMSCs-Exos group (Fig. 7B). Three-dimensional micro-computed tomography (micro-CT) imaging was used to evaluate the effect of Hypo-BMSCs-Exos on the subchondral bone structure of KOA model rats. As shown in Fig. 7C, the integrity of the knee subchondral bone structure in the KOA model group was significantly impaired. In contrast, both Norm-BMSCs-Exos and Hypo-BMSCs-Exos treatment effectively maintained the integrity of the subchondral bone structure. Further observation of sagittal reconstructed images of the knee joint showed that the KOA model group had a significant reduction in subchondral bone mass, with loose trabecular arrangement, fractures, and abnormal morphology. After intervention with Norm-BMSCs-Exos or Hypo-BMSCs-Exos, subchondral bone loss was significantly improved, and the quality of the trabecular structure was maintained (Fig. 7C). Specifically, compared with the KOA model group, both exosome treatments significantly reduced trabecular separation (Tb.Sp) and increased subchondral bone surface area, bone volume/total volume (BV/TV), trabecular number (Tb.N), and trabecular thickness (Tb.Th). Notably, Hypo-BMSCs-Exos showed a more significant repair effect in promoting subchondral bone remodeling than Norm-BMSCs-Exos (Fig. 7D–G).

To further explore the in vivo effect of BMSCs-Exos on chondrocyte catabolism, anabolism, and pro-inflammatory factors, immunohistochemistry was performed on cartilage samples from different treatment groups. The results showed that Hypo-BMSCs-Exos treatment reduced the expression of iNOS, COX2, ADAMTS-5, and MMP-13 in chondrocytes and increased the expression of Collagen II and aggrecan. The regulatory effect of Hypo-BMSCs-Exos on rat chondrocytes was more significant, with statistically significant differences (Fig. 8A and B). These findings indicate that Hypo-BMSCs-Exos have a more potent effect in delaying cartilage degeneration in vivo.

3.7. Intra-articular injection of Hypo-BMSCs-Exos alleviates pain in KOA rats

To evaluate whether Hypo-BMSCs-Exos treatment can alleviate pain in KOA rats, the Von Frey filament test was used to assess mechanical hyperalgesia (Fig. 9A). In the sham operation group, no significant difference in the mechanical pain threshold was observed during the experimental period. In all groups except the sham operation group, the mechanical pain threshold of rats decreased in the first 4 weeks after surgery and then gradually increased. At weeks 6 and 8, the mechanical pain thresholds of the Norm-BMSCs-Exos and Hypo-BMSCs-Exos groups were higher than that of the KOA model group, and the mechanical pain threshold of the Hypo-BMSCs-Exos group was significantly higher.

To further investigate the effect of Hypo-BMSCs-Exos on nociceptive nerve fibers in the subchondral bone, the expression levels of calcitonin gene-related peptide (CGRP) and iNOS proteins in lumbar dorsal root ganglion (DRG) tissue were analyzed. Immunofluorescence (Fig. 9B and C) and Western blotting (Fig. 9D and E) results showed that compared with the sham operation group, the protein levels of CGRP and iNOS in DRG tissue were significantly upregulated in the KOA model group—indicating that KOA rats exhibited a combination of inflammatory and neuropathic pain. In addition, compared with the KOA model group, the protein levels of CGRP and iNOS in the Norm-BMSCs-Exos and Hypo-BMSCs-Exos groups were significantly reduced, suggesting that BMSCs-Exos exert a pain-relieving effect on KOA rats. The reduction in CGRP and iNOS protein levels was more significant in the Hypo-BMSCs-Exos treatment group, indicating that Hypo-BMSCs-Exos are more effective in alleviating pain in KOA rats.

4. Discussion

This study focused on bone marrow mesenchymal stem cell-derived exosomes (BMSCs-Exos) as the core research object. By establishing different culture environments, we separately prepared hypoxia-preconditioned BMSC-derived exosomes (Hypo-BMSCs-Exos) and normoxically cultured BMSC-derived exosomes (Norm-BMSCs-Exos), and systematically investigated the therapeutic effects of these two types of exosomes on knee osteoarthritis (KOA). Through a combination of in vitro cellular experiments and in vivo animal model tests, we found that compared with normoxic culture conditions, a hypoxic culture environment could significantly enhance the biological function of BMSCs-Exos.

In in vitro experiments, Hypo-BMSCs-Exos more effectively inhibited interleukin-1β (IL-1β)-induced chondrocyte apoptosis, reduced cartilage matrix damage, and delayed the senescence process of chondrocytes. In the rat KOA model, after intervention with Hypo-BMSCs-Exos, the defect area of knee joint cartilage tissue in KOA rats was significantly reduced, and pain-related behaviors in rats were notably decreased. These results indicate that Hypo-BMSCs-Exos exert a more potent effect in preventing knee cartilage degeneration and alleviating joint pain. In summary, this study confirms that a hypoxic environment can optimize the function of BMSCs-Exos and improve their therapeutic efficacy against KOA. This research not only provides experimental evidence for an in-depth understanding of the environmental regulation mechanism of BMSCs-Exos but also offers new insights for the clinical treatment and prevention of KOA.

Since the development of regenerative medicine, exosomes derived from different types of mesenchymal stem cells (MSCs) have been regarded as effective tools for treating various refractory clinical diseases [31–33]. It has also been shown that the biological effects of exosomes depend on the culture status of their parent cells. Existing studies have demonstrated that hypoxic preconditioning can improve the therapeutic effect of BMSCs [34,35]. According to previous reports,

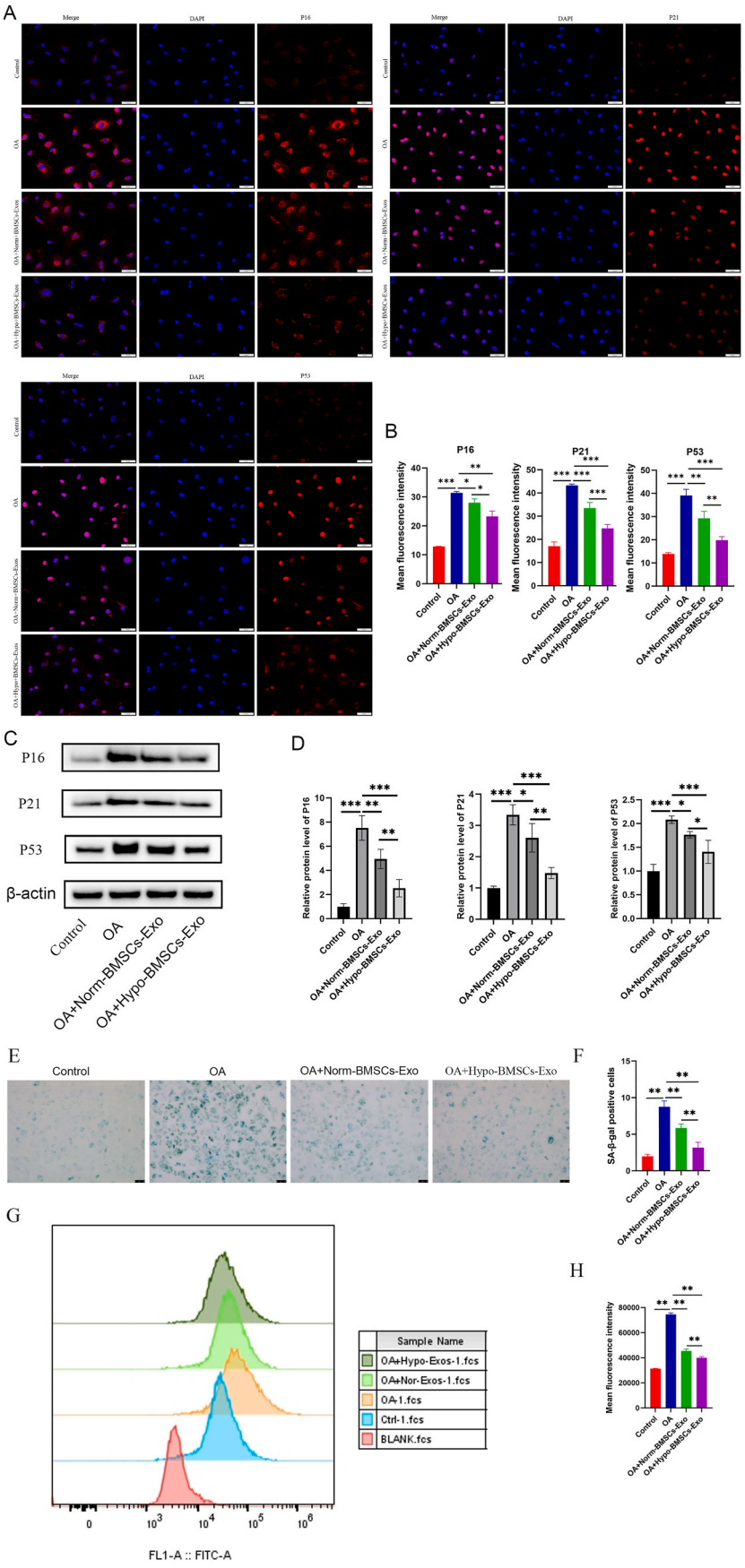

(caption on next page)

Fig. 6. Effects of Hypo-BMSCs-Exos on IL-1β-induced chondrocyte senescence.
A: Immunofluorescence staining revealed changes in p16, p21, and p53 in IL-1β-induced chondrocytes following intervention with Norm-BMSCs-Exos and Hypo-BMSCs-Exos. **B:** Quantitative analysis of immunofluorescence staining. **C:** Western blot detection of p16, p21, and p53 expression in chondrocytes. **D:** Statistical analysis of gray values and relative values for corresponding protein bands. **E:** SA-β-gal activity in chondrocytes across different groups assessed using SA-β-gal staining kit, bar = 75 μm. **F:** Counting and statistical analysis of SA-β-gal positive cells in chondrocytes across groups. **G:** Flow cytometry analysis of mean fluorescence intensity for reactive oxygen species (ROS). **H:** Statistical analysis of ROS expression levels across groups. Results are presented as Mean ± SD. Intergroup statistical significance is indicated as: *P < 0.05, **P < 0.01, ***P < 0.001 (n = 3).

the oxygen concentration in the mammalian bone marrow cavity is relatively low, which differs significantly from the oxygen concentration (21 % oxygen) used for in vitro BMSC culture. Therefore, in this study, BMSCs were exposed to a hypoxic environment, with the expectation that Hypo-BMSCs-Exos would exhibit stronger biological activity. Results of exosome identification showed that culturing BMSCs in a hypoxic environment did not significantly alter the morphology or size of exosomes, but the protein expression level of exosomes was higher. Additionally, BMSCs cultured in a hypoxic environment had a greater advantage in differentiating into chondrocytes and osteoblasts, which may be attributed to the fact that hypoxia is more consistent with the physiological conditions required for BMSC growth and development.

Knee joint cartilage is an avascular tissue that exists in a hypoxic environment, obtaining oxygen and nutrients primarily from superficial synovial blood vessels. Due to the lack of vascular components, articular cartilage develops and maintains its function in a hypoxic microenvironment [36]. Studies have also confirmed that a hypoxic environment can promote chondrogenic differentiation and matrix synthesis [37,38]. With increasing attention paid to the microenvironment by researchers, how to simulate the hypoxic microenvironment within the knee joint to a certain extent has become a current research focus [39]. The results of this study showed that a hypoxic environment can promote the differentiation of BMSCs into chondrocytes, and Hypo-BMSCs-Exos can enhance the expression of aggrecan and Collagen II. Meanwhile, further evidence from the rat KOA model demonstrated that exosomes secreted by BMSCs stimulated by a hypoxic environment can promote the repair of the cartilage layer, highlighting the importance of the hypoxic microenvironment in cartilage homeostasis. Hypoxia can activate the survival mechanism of stem cells, enhance their antioxidant capacity, and promote cell proliferation—all of which help stem cells successfully complete the processes of chondrocyte differentiation and matrix synthesis in a hypoxic environment. The hypoxic environment can simulate the relatively hypoxic physiological state inside the human joint; under this condition, BMSCs are stimulated to differentiate into chondrocytes and promote the secretion of cartilage matrix.

Aging is one of the important risk factors for KOA [40]. Multiple studies have confirmed that cellular senescence plays a key role in the occurrence and development of KOA. Senescent cells have been observed in various structures of knee joint tissue, including cartilage, subchondral bone, and synovium [41]. These cells exhibit several typical characteristics: first, the function of senescent chondrocytes is significantly impaired, with reduced ability to synthesize and secrete the extracellular matrix (ECM); second, they can release a variety of pro-inflammatory factors and matrix-degrading enzymes, thereby altering the local joint microenvironment and accelerating the destruction of the cartilage matrix [42]. Although senescence and KOA can occur as independent processes, it is undeniable that chondrocyte senescence plays an important role in promoting the progression of KOA. Studies have shown that specific clearance of senescent chondrocytes can effectively delay cartilage degeneration and exert a protective effect [43]. In this study, we observed that after stimulation with IL-1β, the expression levels of senescence-related markers (p16, p21, and p53) in chondrocytes increased, and the activity of senescence-associated β-galactosidase (SA-β-gal) and reactive oxygen species (ROS) levels also significantly increased. These results indicate that inflammatory factors can effectively induce chondrocyte senescence, which is consistent with previous mechanistic studies on inflammatory stress promoting cellular senescence [42]. Further experiments showed that intervention with Hypo-BMSCs-Exos significantly delayed the senescence process of chondrocytes induced by IL-1β, as evidenced by downregulated expression of p16, p21, and p53, reduced SA-β-gal activity, and decreased ROS production. Therefore, we suggest that Hypo-BMSCs-Exos may exert a cartilage-protective effect in KOA by reducing ROS release and inhibiting chondrocyte senescence.

Alleviating knee pain is a primary clinical demand of KOA patients. Studies have shown that articular cartilage itself lacks sensory innervation; thus, cartilage damage usually does not directly trigger a pain response. However, the subchondral bone region is rich in sensory nerve endings, and when subjected to noxious stimuli, it may become an important cause of KOA pain [44]. During the course of KOA, chronic pain can induce sensitization of the central and peripheral nervous systems, manifested as mechanical hyperalgesia around the joint—suggesting that neuropathic pain mechanisms may be involved in the occurrence and development of KOA pain [45,46]. As primary sensory neurons, the activation level of dorsal root ganglia (DRG) is closely related to the intensity of sensory stimulation in the innervated area. Multiple studies have confirmed that the expression level of nerve growth factor in peripheral nerve endings and the expression level of calcitonin gene-related peptide (CGRP) in the DRG are positively correlated with pain transmission [47]. Notably, the sensory nerves of the knee joint, especially in the subchondral bone region, mainly project to the lumbar DRG. The results of this study showed that the rat KOA model significantly upregulated the expression of CGRP in the DRG, which is consistent with the conclusions of previous studies.

On the other hand, the mechanism of KOA pain involves a variety of peripheral pain-causing factors, including pro-inflammatory cytokines (e.g., IL-1β, IL-6, TNF-α, iNOS). These mediators participate in pain generation and peripheral sensitization through interaction with sensory nerves [48]. Noxious signals are transmitted to the central nervous system via the dorsal horn of the spinal cord, ultimately forming pain perception in the cerebral cortex. Under stimulation by pro-inflammatory factors, iNOS is rapidly expressed and produces nitric oxide (NO), which triggers an inflammatory cascade and promotes the progression of inflammation. This study found that KOA model rats injected with BMSCs-Exos via the joint cavity exhibited significant improvement in pain-related behaviors. In addition, compared with the KOA group, the protein levels of CGRP and iNOS in the DRG of rats injected with Hypo-BMSCs-Exos were significantly reduced, and the fluorescence intensity of CGRP and iNOS in the DRG was also significantly decreased. These results further indicate that exosome treatment can alleviate both inflammatory and neuropathic pain in OA rats. A possible mechanism for this phenomenon is that Hypo-BMSCs-Exos improve the subchondral bone microenvironment and reduce abnormal innervation, thereby decreasing the activation of nerve endings by noxious stimuli. In conclusion, the study results suggest that Hypo-BMSCs-Exos may have potential therapeutic value in alleviating KOA pain symptoms.

Hypoxia preconditioning not only enhances the release of BMSCs-Exos but also modifies their cargo composition—including specific miRNAs and proteins—thereby augmenting their biological efficacy. Reports indicate that exosomes derived from BMSCs under hypoxic conditions exhibit significantly elevated levels of miR-210-3p and miR-125a-5p [35,49]. Among these, miR-210-3p has been shown to mitigate osteoarthritis progression by targeting TGFBR1 and ID4, thereby suppressing subchondral angiogenesis [50]. Meanwhile, miR-125a-5p promotes chondrocyte migration and is associated with the upregulation of

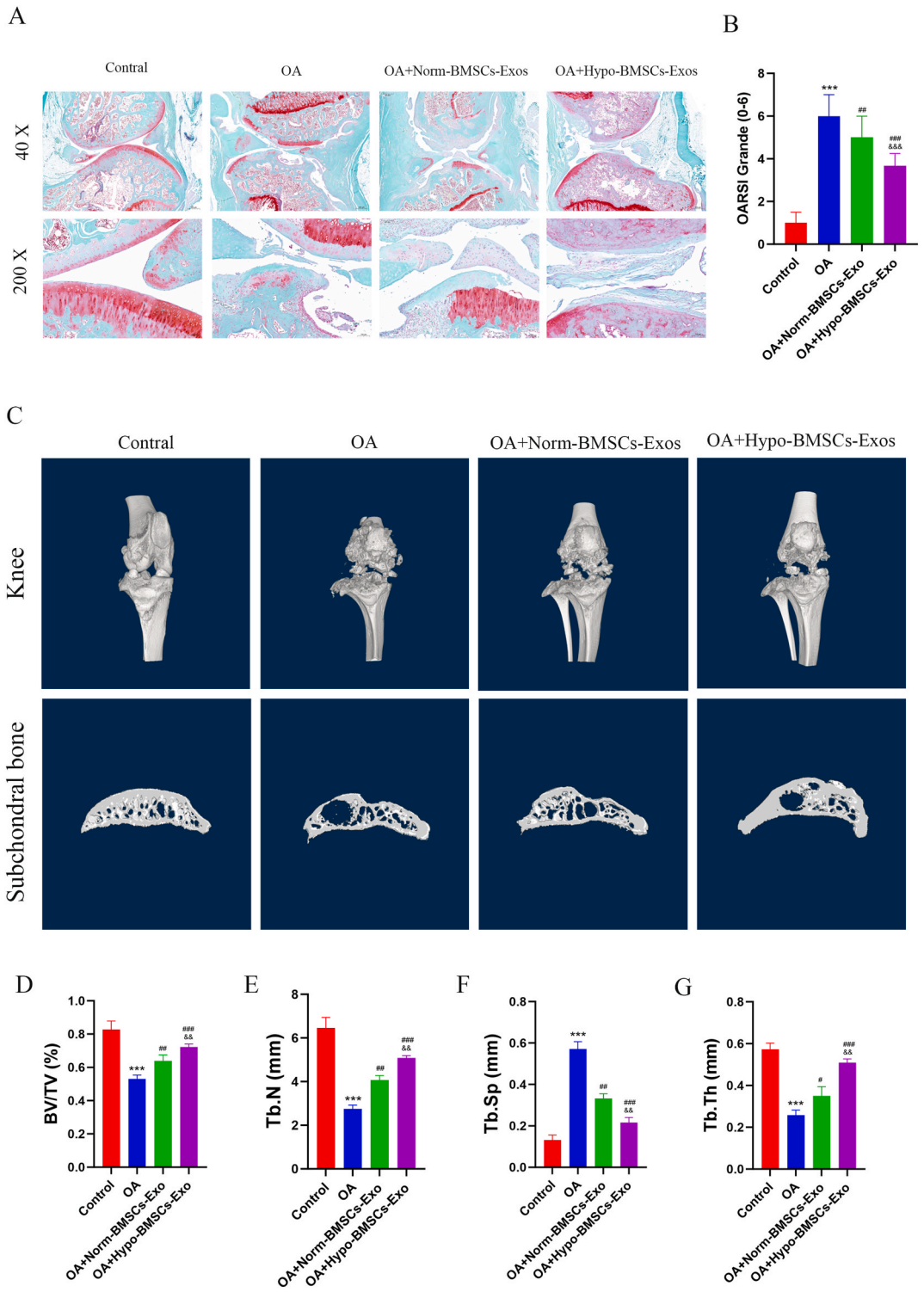

Fig. 7. Intra-articular injection of Hypo-BMSCs-Exo maintains the microstructure of articular cartilage and subchondral bone in KOA rats.
A: Representative histological images of KOA knee cartilage after 8 weeks of intervention, stained with safranin O/fast green. **B:** Progression of cartilage degeneration assessed using the OARSI scoring system. **C:** Three-dimensional reconstructed X-ray micrographs of subchondral bone surfaces (upper panel) and corresponding sagittal microstructures of the tibial subchondral bone (lower panel) in rats from different treatment groups, scale bar = 200 μm. **D–G:** Histomorphometric analysis of three-dimensional subchondral bone images in rats from different groups. All data are expressed as Mean ± SD, with n = 3 per group. Statistical significance between groups is indicated as: $^{*}P < 0.05$, $^{**}P < 0.01$, $^{***}P < 0.001$ compared to control rats; $^{\#}p < 0.05$、$^{\#\#}p < 0.01$、$^{\#\#\#}p < 0.001$ indicate differences compared with OA rats; $^{\&}p < 0.05$、$^{\&\&}p < 0.01$、$^{\&\&\&}p < 0.001$ indicate differences compared with Norm-BMSCs-Exos rats.

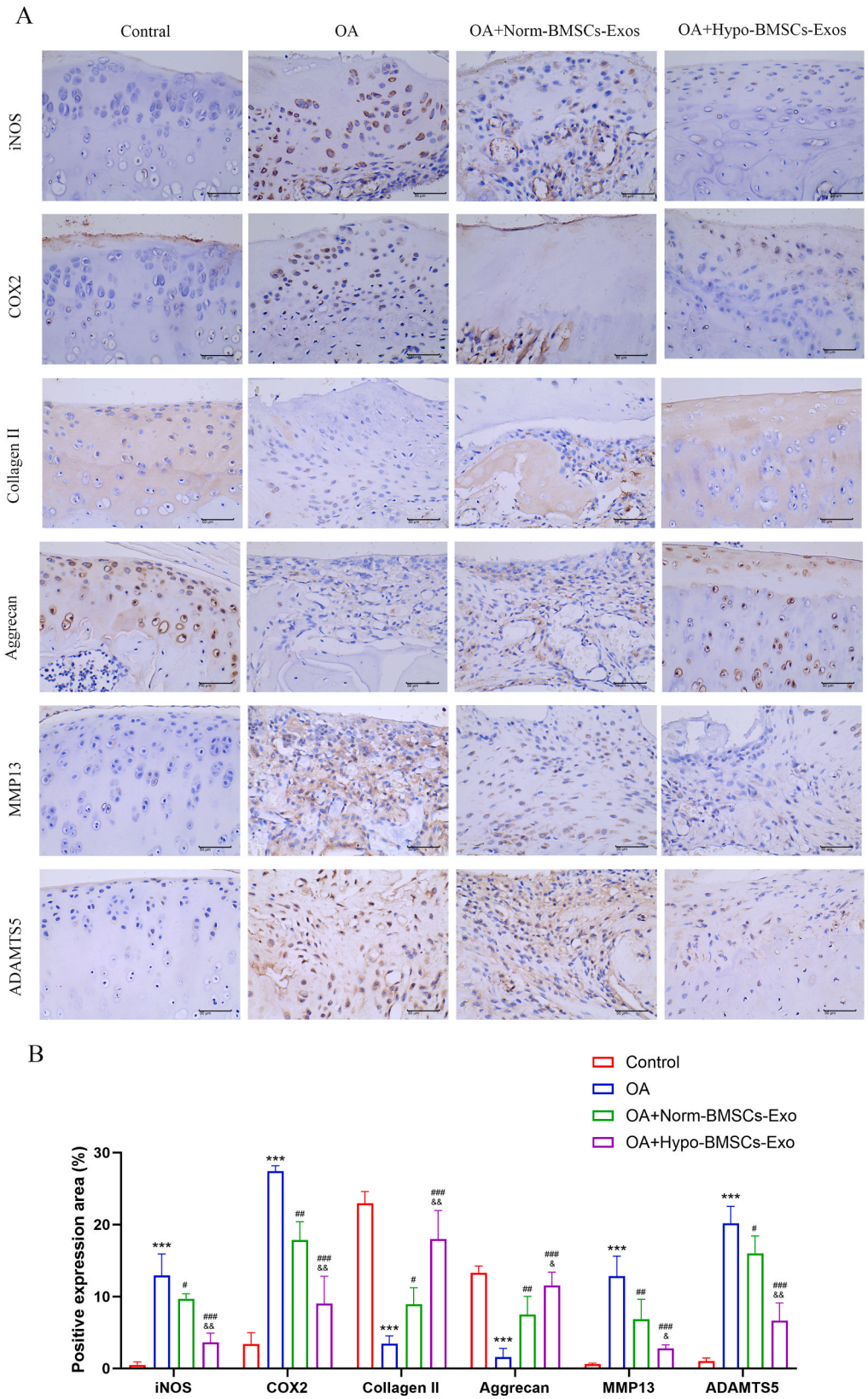

Fig. 8. Intra-articular injection of Hypo-BMSCs-Exo protects articular cartilage from degeneration in KOA rats.
A: Representative images of immunohistochemical staining for iNOS, COX2, Collagen II, Aggrecan, ADAMTS-5, and MMP-13 in cartilage tissue at 8 weeks post-intervention. Scale bar = 50 μm. **B:** Quantitative analysis and statistical evaluation of immunopositive cells. Data are expressed as mean ± standard deviation (SD), with n = 3 per group. Intergroup statistical significance is indicated as: *P < 0.05, **P < 0.01, ***P < 0.001 compared to control rats; $^{\#}p < 0.05$、$^{\#\#}p < 0.01$、$^{\#\#\#}p < 0.001$ indicate differences compared with OA rats; $^{\&}p < 0.05$、$^{\&\&}p < 0.01$、$^{\&\&\&}p < 0.001$ indicate differences compared with Norm-BMSCs-Exos rats.

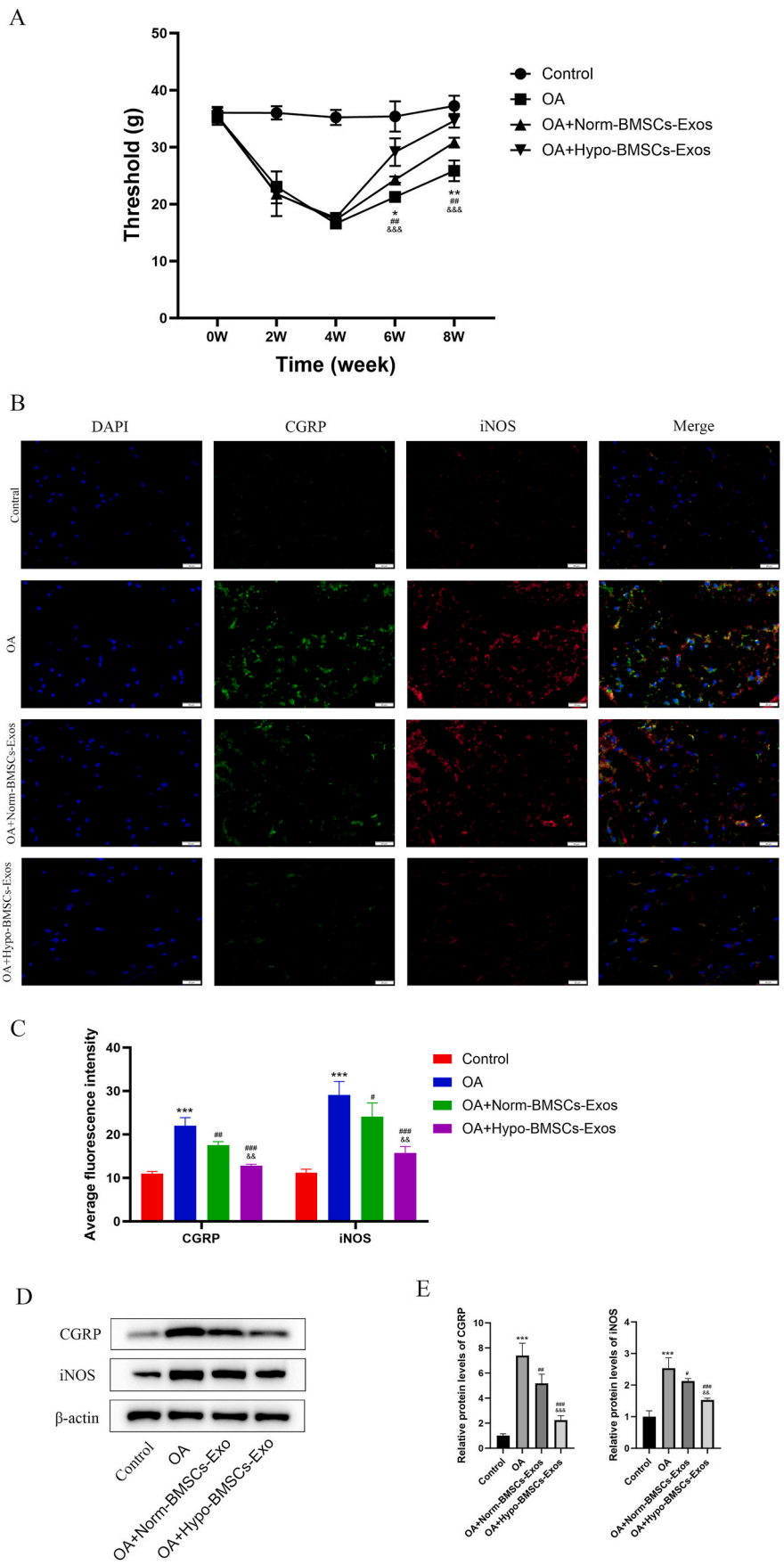

(caption on next page)

Fig. 9. Intra-articular injection of Hypo-BMSCs-Exos alleviates pain in KOA rats.
A: Mechanical hyperalgesia and pain thresholds were assessed using the Von Frey filament test at weeks 2, 4, 6, and 8 post-intervention. **B:** Immunofluorescence staining revealed CGRP and iNOS expression in dorsal root ganglion (DRG) tissue across groups. Scale bar = 20 μm. **C:** Quantitative analysis of CGRP and iNOS immunofluorescence staining. **D:** Western blot analysis of CGRP and iNOS protein expression in DRG tissue across groups. **E:** Statistical analysis of relative gray values for protein bands. All data are expressed as mean ± standard deviation (SD) (n = 3). Statistical significance between groups is indicated as: $^{*}P < 0.05$, $^{**}P < 0.01$, $^{***}P < 0.001$ compared to control rats; $^{\#}p < 0.05$、$^{\#\#}p < 0.01$、$^{\#\#\#}p < 0.001$ indicate differences compared with OA rats; $^{\&}p < 0.05$、$^{\&\&}p < 0.01$、$^{\&\&\&}p < 0.001$ indicate differences compared with Norm-BMSCs-Exos rats.

collagen II, aggrecan, and SOX9, along with downregulation of MMP-13 in vitro. Studies in mouse OA models further confirm that miR-125a-5p attenuates extracellular matrix degradation in chondrocytes [51]. Beyond miRNAs, Hypo-BMSCs-Exos are likely enriched with anti-inflammatory proteins such as TGF-β1 and cartilage-protective factors like IGF-1. Evidence suggests that these proteins stimulate collagen II synthesis and suppress the expression of COX-2 and iNOS in KOA chondrocytes [52–54]. Our BCA assay results, which demonstrated higher total protein content in Hypo-BMSCs-Exos, further support the notion that hypoxia preconditioning promotes protein enrichment within exosomes.

However, this study also has certain limitations: First, only a specific source of rat chondrocyte line was used, and the cell source was relatively single, which may not fully represent the characteristics of chondrocytes from different individuals and different pathological stages. In subsequent studies, multiple cell types will be further investigated to verify the above conclusions. Second, the exact molecular mechanism by which Hypo-BMSCs-Exos improve knee OA cartilage degeneration and joint pain remains unclear; future work should focus on exploring this mechanism through proteomic and transcriptomic analyses to identify key functional components (e.g., specific miRNAs or proteins) in Hypo-BMSCs-Exos that mediate the observed therapeutic effects. Although the dosage and injection frequency employed in this study proved effective, they were determined based on existing literature and preliminary data. A comprehensive investigation into the peripheral administration mechanism, optimal dosage, and minimum effective injection frequency of Hypo-BMSCs-Exos falls beyond the scope of this work. Future studies should systematically evaluate different dosing regimens to establish a clear dose-response relationship and maximize its translational potential.

5. Conclusions

In conclusion, Hypo-BMSCs-Exos exhibit stronger abilities to promote chondrocyte proliferation and delay cellular senescence compared with Norm-BMSCs-Exos. Animal experiments further confirmed that Hypo-BMSCs-Exos can more effectively promote the repair of articular cartilage structure, restore the integrity of subchondral bone, and significantly alleviate KOA-related pain symptoms. This study provides a new potential strategy and experimental basis for the clinical treatment of KOA, and lays a foundation for the further development of cell-free therapeutic approaches targeting KOA.

Consent for publication

All authors have read and agreed to the submitted version of the manuscript.

Ethics approval

All experimental procedures and operations were approved by the Ethics Committee of the Scientific Research Ethics Committee of Qinghai University Affiliated Hospital.(Approval No. SL-2024148).

Data availability statement

The original contributions presented in the study are included in the article/supplementary material. Further inquiries can be directed to the corresponding authors.

Author contributions

All authors made significant contributions to this study. Binbin Zhang and Kewen Li were responsible for the conception and methodology of the study; Binbin Zhang, Chuan Lu, Wenzuo Gu, and Bin Dou conducted the survey and organized the data; Binbin Zhang and Chuan Lu completed the first draft; and Kewen Li reviewed and edited the manuscript. Binbin Zhang, Chuan Lu, Wenzuo Gu, Bin Dou, and Kewen Li gave final approval of the submitted version.

Funding

2024 Provincial and ministerial joint construction of Central Asia high disease causes and prevention of the national key laboratory-Qinghai Workstation Joint Fund (SKL-HIDCA-2024-QH1).

Declaration of competing interest

The authors of this study declare that there are no conflicts of interest.

Acknowledgments

We extend our sincere gratitude to the Laboratory of Qinghai University Affiliated Hospital. At the same time, we would like to express our special thanks to my advisor and fellow students who provided invaluable assistance. Without your support, I would not have been able to successfully complete this research project.

Appendix A. Supplementary data

Supplementary data to this article can be found online at https://doi.org/10.1016/j.reth.2025.101049.

References

[1] Sanchez-Lopez E, Coras R, Torres A, et al. Synovial inflammation in osteoarthritis progression. Nat Rev Rheumatol 2022;18(5):258–75. https://doi.org/10.1038/s41584-022-00749-9.
[2] Panichi V, Costantini S, Grasso M, et al. Innate immunity and synovitis: key players in osteoarthritis progression. Int J Mol Sci 2024;25(22). https://doi.org/10.3390/ijms252212082.
[3] Ren JL, Yang J, Hu W. The global burden of osteoarthritis knee: a secondary data analysis of a population-based study. Clin Rheumatol 2025;44(4):1769–810. https://doi.org/10.1007/s10067-025-07347-6.
[4] Weng Q, Chen Q, Jiang T, et al. Global burden of early-onset osteoarthritis, 1990-2019: results from the Global Burden of Disease Study 2019. Ann Rheum Dis 2024;83(7):915–25. https://doi.org/10.1136/ard-2023-225324.
[5] Onuora S. Which NSAIDs are best for OA treatment? Nat Rev Rheumatol 2021;17(12):707. https://doi.org/10.1038/s41584-021-00716-w.
[6] Chavda S, Rabbani SA, Wadhwa T. Role and effectiveness of intra-articular injection of hyaluronic acid in the treatment of knee osteoarthritis: a systematic review. Cureus 2022;14(4):e24503. https://doi.org/10.7759/cureus.24503.
[7] Skou ST, Roos EM, Laursen MB, et al. A randomized, controlled trial of total knee replacement. N Engl J Med 2015;373(17):1597–606. https://doi.org/10.1056/NEJMoa1505467.
[8] Bindu S, Mazumder S, Bandyopadhyay U. Non-steroidal anti-inflammatory drugs (NSAIDs) and organ damage: a current perspective. Biochem Pharmacol 2020;180:114147. https://doi.org/10.1016/j.bcp.2020.114147.
[9] Qiao X, Yan L, Feng Y, et al. Efficacy and safety of corticosteroids, hyaluronic acid, and PRP and combination therapy for knee osteoarthritis: a systematic review and

network meta-analysis. BMC Muscoskelet Disord 2023;24(1):926. https://doi.org/10.1186/s12891-023-06925-6.
[10] Bayliss LE, Culliford D, Monk AP, et al. The effect of patient age at intervention on risk of implant revision after total replacement of the hip or knee: a population-based cohort study. Lancet 2017;389(10077):1424–30. https://doi.org/10.1016/S0140-6736(17)30059-4.
[11] Zou XF, Zhang BZ, Qian WW, et al. Bone marrow mesenchymal stem cells in treatment of peripheral nerve injury. World J Stem Cell 2024;16(8):799–810. https://doi.org/10.4252/wjsc.v16.i8.799.
[12] Kim Do Jung, Hahn Hyung Min, Youn Young-Nam, et al. Adipose derived stromal vascular fraction and mesenchymal stem cells improve angiogenesis in a Rat Hindlimb Ischaemia Model. Eur J Vasc Endovasc Surg Off J Europ Soc Vascular Surg 2023. https://doi.org/10.1016/j.ejvs.2023.11.036.
[13] Zhang X, Liu T, Ran C, et al. Immunoregulatory paracrine effect of mesenchymal stem cells and mechanism in the treatment of osteoarthritis. Front Cell Dev Biol 2024;12:1411507. https://doi.org/10.3389/fcell.2024.1411507.
[14] Song Q, Zhou A, Cheng W, et al. Bone marrow mesenchymal stem cells-derived exosomes inhibit apoptosis of pulmonary microvascular endothelial cells in COPD mice through miR-30b/Wnt5a pathway. Int J Nanomed 2025;20:1191–211. https://doi.org/10.2147/IJN.S487097.
[15] Donghyeon Yoo, Young Se, Jung Dabin, Go, et al. Functionalized extracellular vesicles of mesenchymal stem cells for regenerative medicine. J Nanobiotechnol 2025;23.
[16] Zhang Y, Qi G, Yan Y, et al. Exosomes derived from bone marrow mesenchymal stem cells pretreated with decellularized extracellular matrix enhance the alleviation of osteoarthritis through miR-3473b/phosphatase and tensin homolog axis. J Gene Med 2023;25(8):e3510. https://doi.org/10.1002/jgm.3510.
[17] Liu C, Li Y, Yang Z, et al. Kartogenin enhances the therapeutic effect of bone marrow mesenchymal stem cells derived exosomes in cartilage repair. Nanomedicine (Lond) 2020;15(3):273–88. https://doi.org/10.2217/nnm-2019-0208.
[18] Wang Y, Hu K, Liao C, et al. Exosomes-shuttled lncRNA SNHG7 by bone marrow mesenchymal stem cells alleviates osteoarthritis through targeting miR-485-5p/FSP1 axis-mediated chondrocytes ferroptosis and inflammation. Tissue Eng Regen Med 2024;21(8):1203–16. https://doi.org/10.1007/s13770-024-00668-8.
[19] Luo Z, Wu F, Xue E, et al. Hypoxia preconditioning promotes bone marrow mesenchymal stem cells survival by inducing HIF-1α in injured neuronal cells derived exosomes culture system. Cell Death Dis 2019;10(2):134. https://doi.org/10.1038/s41419-019-1410-y.
[20] Lou C, Jiang H, Lin Z, et al. MiR-146b-5p enriched bioinspired exosomes derived from fucoidan-directed induction mesenchymal stem cells protect chondrocytes in osteoarthritis by targeting TRAF6. J Nanobiotechnol 2023;21(1):486. https://doi.org/10.1186/s12951-023-02264-9.
[21] Zhou PH, Liu SQ, Peng H. The effect of hyaluronic acid on IL-1beta-induced chondrocyte apoptosis in a rat model of osteoarthritis. J Orthop Res 2008;26(12):1643–8. https://doi.org/10.1002/jor.20683.
[22] Yu J, Yin S, Zhang W, et al. Hypoxia preconditioned bone marrow mesenchymal stem cells promote liver regeneration in a rat massive hepatectomy model. Stem Cell Res Ther 2013;4(4):83. https://doi.org/10.1186/scrt234.
[23] Théry C, Amigorena S, Raposo G, et al. Isolation and characterization of exosomes from cell culture supernatants and biological fluids. Curr Protoc Cell Biol 2006. https://doi.org/10.1002/0471143030.cb0322s30 [Chapter 3]:Unit 3.22.
[24] Mende LK, Kuthati Y, Wong CS. Curcumin and vitamin D supplement attenuates knee osteoarthritis progression in ACLT + MMx rat model: effect on cartilage protection and pain reduction. Nutrients 2025;17(2). https://doi.org/10.3390/nu17020349.
[25] Besler BA, Schadow JE, Durongbhan P, et al. Quantitative measures of bone shape, cartilage morphometry and joint alignment are associated with disease in an ACLT and MMx rat model of osteoarthritis. Bone 2021;146:115903. https://doi.org/10.1016/j.bone.2021.115903.
[26] Guo H, Yin W, Zou Z, et al. Quercitrin alleviates cartilage extracellular matrix degradation and delays ACLT rat osteoarthritis development: an in vivo and in vitro study. J Adv Res 2021;28:255–67. https://doi.org/10.1016/j.jare.2020.06.020.
[27] Cheng S, Xu X, Wang R, et al. Chondroprotective effects of bone marrow mesenchymal stem cell-derived exosomes in osteoarthritis. J Bioenerg Biomembr 2024;56(1):31–44. https://doi.org/10.1007/s10863-023-09991-6.
[28] Pang L, Xiang L, Chen G, et al. In-situ hydrogen-generating injectable short fibers for osteoarthritis treatment by alleviating oxidative stress. Acta Biomater 2024;188:406–19. https://doi.org/10.1016/j.actbio.2024.09.008.
[29] Nwosu LN, Mapp PI, Chapman V, et al. Blocking the tropomyosin receptor kinase A (TrkA) receptor inhibits pain behaviour in two rat models of osteoarthritis. Ann Rheum Dis 2016;75(6):1246–54. https://doi.org/10.1136/annrheumdis-2014-207203.
[30] Vermeirsch H, Biermans R, Salmon PL, et al. Evaluation of pain behavior and bone destruction in two arthritic models in Guinea pig and rat. Pharmacol Biochem Behav 2007;87(3):349–59. https://doi.org/10.1016/j.pbb.2007.05.010.
[31] Jiao YR, Chen KX, Tang X, et al. Exosomes derived from mesenchymal stem cells in diabetes and diabetic complications. Cell Death Dis 2024;15(4):271. https://doi.org/10.1038/s41419-024-06659-w.
[32] Liu P, Yang S, Shao X, et al. Mesenchymal stem cells-derived exosomes alleviate acute lung injury by inhibiting alveolar macrophage pyroptosis. Stem Cells Transl Med 2024;13(4):371–86. https://doi.org/10.1093/stcltm/szad094.
[33] Jia S, Yang T, Gao S, et al. Exosomes from umbilical cord mesenchymal stem cells ameliorate intervertebral disc degeneration via repairing mitochondrial dysfunction. J Orthop Translat 2024;46:103–15. https://doi.org/10.1016/j.jot.2023.10.004.
[34] Tian H, Yang X, Zhao J, et al. Hypoxia-preconditioned bone marrow mesenchymal stem cells improved cerebral collateral circulation and stroke outcome in mice. Arterioscler Thromb Vasc Biol 2023;43(7):1281–94. https://doi.org/10.1161/ATVBAHA.122.318559.
[35] Wang M, Zheng Y, Hao Q, et al. Hypoxic BMSC-derived exosomal miR-210-3p promotes progression of triple-negative breast cancer cells via NFIX-Wnt/β-catenin signaling axis. J Transl Med 2025;23(1):39. https://doi.org/10.1186/s12967-024-05947-5.
[36] Lafont JE. Lack of oxygen in articular cartilage: consequences for chondrocyte biology. Int J Exp Pathol 2010;91(2):99–106. https://doi.org/10.1111/j.1365-2613.2010.00707.x.
[37] Okada K, Mori D, Makii Y, et al. Hypoxia-inducible factor-1 alpha maintains mouse articular cartilage through suppression of NF-κB signaling. Sci Rep 2020;10(1):5425. https://doi.org/10.1038/s41598-020-62463-4.
[38] Ichimaru S, Nakagawa S, Arai Y, et al. Hypoxia potentiates anabolic effects of exogenous hyaluronic acid in rat articular cartilage. Int J Mol Sci 2016;17(7). https://doi.org/10.3390/ijms17071013. null.
[39] Liu K, Zhang B, Zhang X. Promoting articular cartilage regeneration through microenvironmental regulation. J Immunol Res 2024;2024:4751168. https://doi.org/10.1155/2024/4751168.
[40] Cui A, Li H, Wang D, et al. Global, regional prevalence, incidence and risk factors of knee osteoarthritis in population-based studies. eClinicalMedicine 2020:100587. https://doi.org/10.1016/j.eclinm.2020.100587. 29-30.
[41] Xie J, Wang Y, Lu L, et al. Cellular senescence in knee osteoarthritis: molecular mechanisms and therapeutic implications. Ageing Res Rev 2021;70:101413. https://doi.org/10.1016/j.arr.2021.101413.
[42] Greene MA, Loeser RF. Aging-related inflammation in osteoarthritis. Osteoarthr Cartil 2015;23(11):1966–71. https://doi.org/10.1016/j.joca.2015.01.008.
[43] Jeon OH, Kim C, Laberge RM, et al. Local clearance of senescent cells attenuates the development of post-traumatic osteoarthritis and creates a pro-regenerative environment. Nat Med 2017;23(6):775–81. https://doi.org/10.1038/nm.4324.
[44] Dieppe PA, Lohmander LS. Pathogenesis and management of pain in osteoarthritis. Lancet 2005;365(9463):965–73. https://doi.org/10.1016/S0140-6736(05)71086-2.
[45] Zolio L, Lim KY, McKenzie JE, et al. Systematic review and meta-analysis of the prevalence of neuropathic-like pain and/or pain sensitization in people with knee and hip osteoarthritis. Osteoarthr Cartil 2021;29(8):1096–116. https://doi.org/10.1016/j.joca.2021.03.021.
[46] Bevilaqua-Grossi D, Zanin M, Benedetti C, et al. Thermal and mechanical pain sensitization in patients with osteoarthritis of the knee. Physiother Theory Pract 2019;35(2):139–47. https://doi.org/10.1080/09593985.2018.1441930.
[47] Aso K, Walsh DA, Wada H, et al. Time course and localization of nerve growth factor expression and sensory nerve growth during progression of knee osteoarthritis in rats. Osteoarthr Cartil 2022;30(10):1344–55. https://doi.org/10.1016/j.joca.2022.07.003.
[48] Aso K, Shahtaheri SM, Hill R, et al. Associations of symptomatic knee osteoarthritis with histopathologic features in subchondral bone. Arthritis Rheumatol 2019;71(6):916–24. https://doi.org/10.1002/art.40820ns [products referred to in the content].
[49] Jia-Chen, Zuo, Jun Liang, Nan Hu, et al. Hypoxia preconditioned MSC exosomes attenuate high-altitude cerebral edema via the miR-125a-5p/RTEF-1 axis to protect vascular endothelial cells. Bioact Mater 2025;52:541–63.
[50] Tang H, Zhu W, Cao L, et al. miR-210-3p protects against osteoarthritis through inhibiting subchondral angiogenesis by targeting the expression of TGFBR1 and ID4. Front Immunol 2022;13:982278. https://doi.org/10.3389/fimmu.2022.982278.
[51] Xia Q, Wang Q, Lin F, et al. miR-125a-5p-abundant exosomes derived from mesenchymal stem cells suppress chondrocyte degeneration via targeting E2F2 in traumatic osteoarthritis. Bioengineered 2021;12(2):11225–38. https://doi.org/10.1080/21655979.2021.1995580.
[52] Abd El-Aleem SA, Mohammed HH, Saber EA, et al. Mutual inter-regulation between iNOS and TGF-β1: possible molecular and cellular mechanisms of iNOS in wound healing. Biochim Biophys Acta Mol Basis Dis 2020;1866(10):165850. https://doi.org/10.1016/j.bbadis.2020.165850.
[53] Kim MD, Bengtson CD, Yoshida M, et al. Losartan ameliorates TGF-β1-induced CFTR dysfunction and improves correction by cystic fibrosis modulator therapies. J Clin Investig 2022;132(11). https://doi.org/10.1172/JCI155241.
[54] Studer RK, Decker K, Melhem S, et al. Nitric oxide inhibition of IGF-1 stimulated proteoglycan synthesis: role of cGMP. J Orthop Res 2003;21(5):914–21. https://doi.org/10.1016/S0736-0266(03)00029-9.